NASA TECHNICAL NOTE

NASA TN D-6780

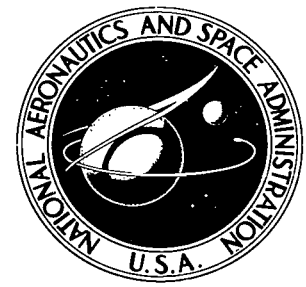

INVISCID ANALYSIS OF JET INJECTION BETWEEN TWO MOVING STREAMS

by Marvin E. Goldstein and Robert Siegel

Lewis Research Center
Cleveland, Ohio 44135

NATIONAL AERONAUTICS AND SPACE ADMINISTRATION • WASHINGTON, D. C. • APRIL 1972

1. Report No.	2. Government Accession No.	3. Recipient's Catalog No.
NASA TN D-6780		

4. Title and Subtitle
INVISCID ANALYSIS OF JET INJECTION BETWEEN TWO MOVING STREAMS

5. Report Date
April 1972

6. Performing Organization Code

7. Author(s)
Marvin E. Goldstein and Robert Siegel

8. Performing Organization Report No.
E-6583

9. Performing Organization Name and Address
Lewis Research Center
National Aeronautics and Space Administration
Cleveland, Ohio 44135

10. Work Unit No.
136-13

11. Contract or Grant No.

12. Sponsoring Agency Name and Address
National Aeronautics and Space Administration
Washington, D. C. 20546

13. Type of Report and Period Covered
Technical Note

14. Sponsoring Agency Code

15. Supplementary Notes

16. Abstract

An analytical method is developed for determining the flow interaction when a two-dimensional jet is injected between two moving streams. The jet is flowing out of a channel and is turned as it enters between the external streams. The local velocity variation resulting from the flow interaction provides a static pressure variation along the jet bounding streamlines that is a priori unknown. Hence, the flow must be obtained by coupling the three flow regions (the jet and the free stream on either side) along the jet boundaries. Both external streams have the same total pressure, which is different from that in the jet. The solution is for the condition that the total pressure in the jet does not differ from the free-stream value by a large amount compared with the free-stream dynamic head. Results are given for the shape of the jet boundaries for various injection configurations.

17. Key Words (Suggested by Author(s))	18. Distribution Statement
Jet injection Jet interaction with stream Inviscid flow Conformal mapping	Unclassified - unlimited

19. Security Classif. (of this report)	20. Security Classif. (of this page)	21. No. of Pages	22. Price*
Unclassified	Unclassified	56	$3.00

* For sale by the National Technical Information Service, Springfield, Virginia 22151

CONTENTS

INVISCID ANALYSIS OF JET INJECTION BETWEEN TWO MOVING STREAMS

by Marvin E. Goldstein and Robert Siegel

Lewis Research Center

SUMMARY

An analytical method was developed for determining the flow characteristics of a two-dimensional jet injected between two moving streams. The jet is flowing out of a channel and is turned as it enters into the main stream flow. As a result, the flow field consists of three regions: the jet, and the main stream on either side of it. In the solution, these regions must be coupled along the two dividing streamline boundaries. The velocity variations along these streamlines produce static pressure variations along them, which introduces a complexity not considered in the usual free streamline analysis of jets. Both external streams have the same total pressure, which is different from that in the jet. The solution is obtained for conditions when the total pressure in the jet does not differ from the free-stream value by a large amount compared with the free-stream dynamic head. Results are obtained for the shape of the jet bounding streamlines as a function of the injection geometry and as a function of the total pressure in the jet relative to that in the free stream.

INTRODUCTION

There are various situations where a stream of fluid is injected into a moving stream of a similar fluid (fig. 1). Examples are the discharge of water into a river, gas blown from an exhaust into the wind, and the injection of gaseous fuel into a stream of oxidant. If, for purposes of analysis, the configuration is approximated as two dimensional, the jet region is bounded on both sides by the outer stream flow. Any turning in the flow produces a variable pressure along both jet boundaries, a feature not taken into account in classical free-jet analyses, where the external flow is usually at rest and hence at uniform static pressure. In reference 1 an inviscid two-dimensional jet was considered exiting from a slot and interacting with a crossflow along one of the jet boundaries. The present report is a further development of the analytical method to include a matching of a jet with an external flow along both jet boundaries. As a result of the inviscid

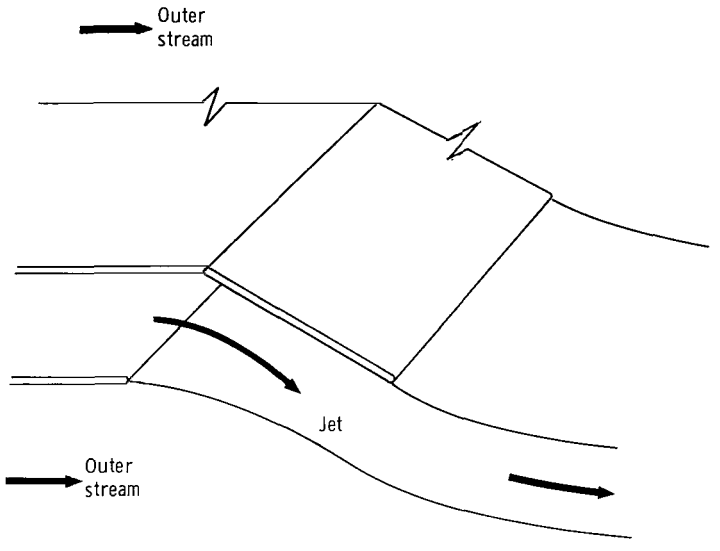

(a) Flow turned and contracted.

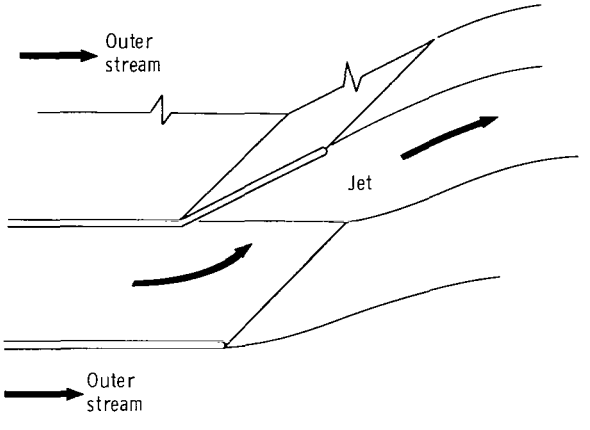

(b) Flow turned and expanded.

Figure 1. - Flow configuration.

assumption the flow patterns are expected to be valid near the jet outlet, where mixing effects are small.

The analysis also accounts for the total pressure in the jet being different from the total pressure in the outer stream. The difference between these total pressures must, however, not be too large compared with the dynamic pressure head of the undisturbed external stream. The problem is solved by expanding the solutions asymptotically in this normalized difference in total pressures.

The zeroth-order solution in the asymptotic expansion corresponds to equal total pressures in jet and stream, and the corresponding solution is obtained by a conventional conformal mapping method. When the total pressures are different, the jet boundaries

will shift away from the zeroth-order streamlines. In the solution method the conditions along these boundaries are transformed to the known zeroth-order boundaries.

The flow configurations studied allow for turning and either contracting or expanding the injected stream as it enters the main stream flow, as shown in figures 1(a) and (b). Results are given for the shape of the jet free streamlines for these configurations for various values of such geometric parameters as the amount of turning.

ANALYSIS

Formulation and Boundary Conditions

It will be assumed that the flow is inviscid, incompressible, and irrotational. The notation describing the jet configuration is illustrated in figure 2(a), which corresponds

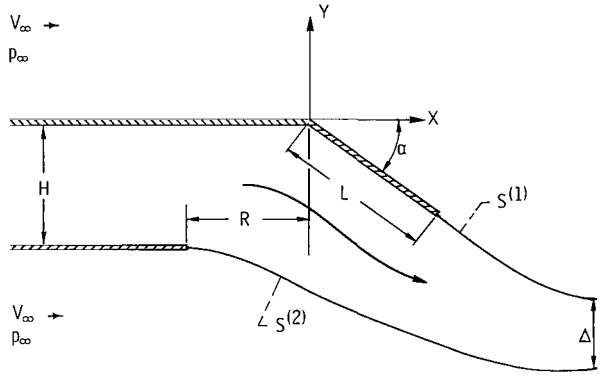

(a) Physical plane (Z-plane).

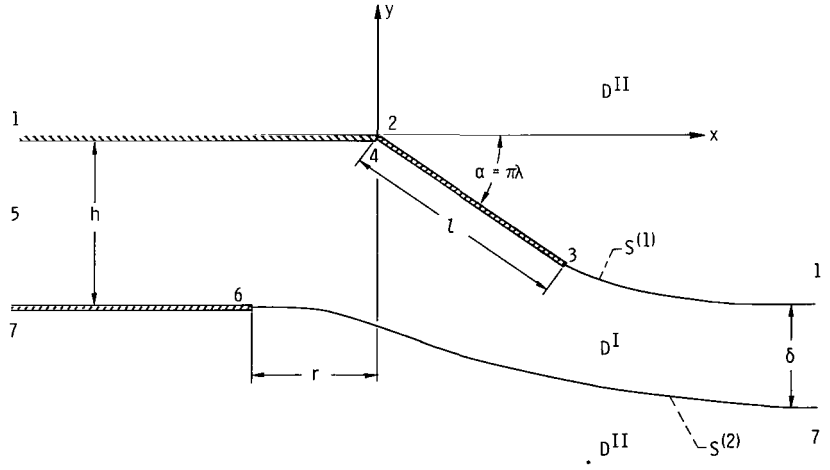

(b) Dimensionless physical plane (z-plane).

Figure 2. - Flow geometry and nomenclature.

to figure 1(a). For the geometry in figure 1(b) the plate angle α would be negative. The analysis is limited to the condition where the difference between the total pressure in the jet P_j and the total pressure in the main stream P_∞ is not too large, so that $|\epsilon| \ll 1$ where

$$\epsilon \equiv \frac{P_j - P_\infty}{\frac{1}{2}\rho V_\infty^2} \tag{1}$$

and ρ is the density of the fluid, and V_∞ is the velocity of the main stream at infinity. (All symbols are defined in the appendix.)

Let b be a convenient reference length which will be specified in the course of the analysis. The X- and Y-components of the velocity, U and V, respectively, are made dimensionless by V_∞; and the stream function Ψ and the velocity potential Φ are made dimensionless by $V_\infty b$. Thus, the dimensionless quantities u, v, ψ, and φ are defined by

$$u = \frac{U}{V_\infty}$$

$$v = \frac{V}{V_\infty}$$

$$\psi = \frac{\Psi}{V_\infty b}$$

$$\varphi = \frac{\Phi}{V_\infty b}$$

The dimensionless complex conjugate velocity ζ and the dimensionless complex potential w are defined, as usual, by

$$\zeta = u - iv$$

and

$$w = \varphi + i\psi$$

With all lengths made dimensionless by b (i.e., $x = X/b$, $y = Y/b$, $l = L/b$, $\delta = \Delta/b$,

$h = H/b$, and $r = R/b$), the flow configuration is shown in the dimensionless physical plane (with the complex variable z defined by $z = x + iy$) in figure 2(b).

The stream of fluid issuing from the orifice formed by the walls $\overset{\frown}{345}$ and $\overset{\frown}{56}$ (fig. 2(b)) meets the main stream at the points 3 and 6 and forms the common streamlines which are denoted by $S^{(1)}$ and $S^{(2)}$ in figure 2. Points on the streamline $S^{(1)}$ are denoted by $z^{(1)} = x^{(1)} + iy^{(1)}$, and points on the streamline $S^{(2)}$ are denoted by $z^{(2)} = x^{(2)} + iy^{(2)}$.

In order to satisfy the requirement that there be no discontinuities in static pressure anywhere within the flow field, it is necessary (as shown in ref. 1) to allow the velocity to be discontinuous across $S^{(1)}$ and $S^{(2)}$. For this reason the streamlines $S^{(1)}$ and $S^{(2)}$ will be called slip lines. The region within the jet and the orifice is denoted by D^{I}, and the remaining region of the flow (i.e., the main stream) by D^{II}. Since the velocity (and, as a consequence, the velocity potential) is discontinuous across $S^{(1)}$ and $S^{(2)}$, it is convenient to use a superscript I to denote the flow quantities inside the jet (i.e., in D^{I}) and a superscript II to denote those in the main stream. Thus,

$$\zeta(z) = \begin{cases} \zeta^{I}(z) & \text{for } z \in D^{I} \\ \zeta^{II}(z) & \text{for } z \in D^{II} \end{cases}$$

and

$$w(z) = \begin{cases} w^{I}(z) & \text{for } z \in D^{I} \\ w^{II}(z) & \text{for } z \in D^{II} \end{cases}$$

Then ζ^{I} and w^{I} are holomorphic in the interior of D^{I}, and ζ^{II} and w^{II} are holomorphic in the interior of D^{II}.

A repetition of the argument given in reference 1 shows that Bernoulli's equation implies

$$\left|\zeta^{I}\left(z^{(1)}\right)\right|^2 - \left|\zeta^{II}\left(z^{(1)}\right)\right|^2 = \frac{P_j - P_\infty}{\frac{1}{2}\rho V_\infty^2} = \epsilon \tag{2}$$

for every point $z^{(1)}$ of $S^{(1)}$ and

$$\left|\zeta^{I}\left(z^{(2)}\right)\right|^2 - \left|\zeta^{II}\left(z^{(2)}\right)\right|^2 = \epsilon \tag{3}$$

for every point $z^{(2)}$ of $S^{(2)}$. Since $S^{(1)}$ and $S^{(2)}$ are both common streamlines, it is clear that

$$\mathcal{I}m\, w^{I}\left(z^{(1)}\right) = \mathcal{I}m\, w^{II}\left(z^{(1)}\right) = \text{constant}$$

$$\mathcal{I}m\, w^{I}\left(z^{(2)}\right) = \mathcal{I}m\, w^{II}\left(z^{(2)}\right) = \text{constant}$$

Moreover, the arbitrariness in the level of w can be partially removed by choosing one of these constants to be zero (ref. 2). Hence, we can put

$$\mathcal{I}m\, w^{I}\left(z^{(1)}\right) = \mathcal{I}m\, w^{II}\left(z^{(1)}\right) = 0 \tag{4}$$

$$\mathcal{I}m\, w^{I}\left(z^{(2)}\right) = \mathcal{I}m\, w^{II}\left(z^{(2)}\right) = \psi^{(2)} \tag{5}$$

where $\psi^{(2)}$ is a real constant.

The remaining arbitrariness in w can be removed by choosing (at the end point of the flap in fig. 2(b))

$$w^{I}(l e^{-i\pi\lambda}) = w^{II}(l e^{-i\pi\lambda}) = 0 \tag{6}$$

The condition imposed on the velocity at infinity is (in view of the manner of nondimensionalization)

$$\zeta^{II}(z) \to 1 \quad \text{for } z \to \text{point 1 and } z \to \text{point 7} \tag{7}$$

The remaining boundary conditions are that the normal component of the velocity vanish on the solid boundaries. These conditions are sufficient to completely determine the solution. They are summarized here for convenient reference:

$$
\left.
\begin{aligned}
&\left|\zeta^{I}(z)\right|^2 - \left|\zeta^{II}(z)\right|^2 = \epsilon \\
&\mathcal{Im}\ w^{I}(z) = \mathcal{Im}\ w^{II}(z) = 0
\end{aligned}
\right\} \text{ for } z \in S^{(1)}
$$

$$
\left.
\begin{aligned}
&\left|\zeta^{I}(z)\right|^2 - \left|\zeta^{II}(z)\right|^2 = \epsilon \\
&\mathcal{Im}\ w^{I}(z) = \mathcal{Im}\ w^{II}(z) = \psi^{(2)}
\end{aligned}
\right\} \text{ for } z \in S^{(2)}
$$

$$
\mathcal{Im}\ \zeta^{I}(z) = 0 \quad \text{for } z \in \widehat{45} \text{ and } z \in \widehat{56}
$$

$$
\mathcal{Im}\ \zeta^{II}(z) = 0 \quad \text{for } z \in \widehat{12} \text{ and } z \in \widehat{67}
$$

$$
\arg \zeta^{I}(z) = \pi\lambda \quad \text{for } z \in \widehat{34}
$$

$$
\arg \zeta^{II}(z) = \pi\lambda \quad \text{for } z \in \widehat{23}
$$

(8)

Asymptotic Expansions

For small values of ϵ the functions ζ^{I}, ζ^{II}, w^{I}, and w^{II} can be expanded in an asymptotic power series in ϵ. In view of the fact that the shape of each slip lines depends on ϵ, these expansions imply that the coordinates of $S^{(1)}$, $S^{(2)}$ $z^{(1)}$, $z^{(2)}$, as well as the asymptotic jet width δ, must also be expanded in powers of ϵ. Hence,

$$
\left.
\begin{aligned}
\zeta^{I} &= \zeta_0 + \epsilon\zeta_1^{I} + \cdots \\
\zeta^{II} &= \zeta_0 + \epsilon\zeta_1^{II} + \cdots \\
w^{I} &= w_0 + \epsilon w_1^{I} + \cdots \\
w^{II} &= w_0 + \epsilon w_1^{II} + \cdots \\
z^{(1)} &= z_0^{(1)} + \epsilon z_1^{(1)} + \cdots \\
z^{(2)} &= z_0^{(2)} + \epsilon z_1^{(2)} + \cdots \\
\delta &= \delta_0 + \epsilon\delta_1 + \cdots \\
\psi^{(2)} &= \psi_0^{(2)} + \epsilon\psi_1^{(2)} + \cdots
\end{aligned}
\right\}
$$

(9)

As pointed out in reference 1 the expansion of $z^{(1)}$ and $z^{(2)}$ does not imply that the complex variable z itself is being expanded. It is shown in reference 1 that the coefficients in the expansions of ζ^{I} and ζ^{II} are related to those in the expansions of w^{I} and w^{II}, respectively, by

$$\left.\begin{aligned} \zeta_0 &= \frac{dw_0}{dz} \\ \zeta_1^{I} &= \frac{dw_1^{I}}{dz} \\ \zeta_1^{II} &= \frac{dw_1^{II}}{dz} \\ &\vdots \end{aligned}\right\} \tag{10}$$

The reason for omitting the superscript I or II in the zeroth-order terms of the first four expansions is that (as will be shown subsequently) the zeroth-order solutions are not discontinuous across the curves $S^{(1)}$ and $S^{(2)}$. Hence, there is a single function ζ_0 which is holomorphic in the entire flow field (of course, the same is true of w_0).

The reference length b will now be chosen in such a way that $\delta_0 = 1$. Thus, b is the zeroth-order asymptotic thickness (at ∞) of the jet. This is denoted symbolically by putting $b = \Delta_0$. The second last expansion (9) is then

$$\delta = 1 + \epsilon\delta_1 + O(\epsilon^2) \ldots \tag{11}$$

Zeroth-Order Solution

Boundary conditions for zeroth-order solution. - When the expansions (eq. (9)) are substituted into the boundary conditions (eqs. (7) and (8)) and only the zeroth-order terms are retained, the following boundary conditions for the zeroth-order solution are obtained. First, the first two boundary conditions in equation (8) show, as has already been anticipated, that the zeroth-order solution must be continuous across the slip lines and, hence, is characterized by functions which are holomorphic everywhere within the flow field. The remaining conditions show that

$$\left.\begin{aligned} w_0(\ell e^{-i\pi\lambda}) &= 0 \\ \mathcal{I}m\ w_0\left(z_0^{(1)}\right) &= 0 \end{aligned}\right\} \tag{12}$$

$$\mathcal{I}m\ w_0\left(z_0^{(2)}\right) = \psi_0^{(2)} \tag{13}$$

$$\mathcal{I}m\ \zeta_0(z) = 0 \quad \text{for } z \in \widehat{45},\ z \in \widehat{56},\ z \in \widehat{12}, \text{ and } z \in \widehat{67} \tag{14}$$

$$\arg \zeta_0(z) = \pi\lambda \quad \text{for } z \in \widehat{23} \text{ and } z \in \widehat{34} \tag{15}$$

$$\zeta_0(z) \to 1 \quad \text{for } z \to \text{point 1 and } z \to \text{point 7} \tag{16}$$

The conditions (12) and (13) merely serve to identify the coordinates $z_0^{(1)}$ and $z_0^{(2)}$ of the zeroth-order streamlines emanating from points 3 and 6 in figure 2(b) and to indicate that the streamline emanating from point 3 is to be taken as the zero streamline.

Now the change in the stream function across the jet must be equal to the volume flow rate through the jet. Hence, if Q_0 denotes the dimensionless zeroth-order volume flow through the jet, and since equation (13) shows that $-\psi_0^{(2)}$ is the zeroth-order change in the stream function across the jet, it is clear from the definition of the stream function that $Q_0 = -\psi_0^{(2)}$.

However, the boundary condition (16) shows that far downstream in the jet the zeroth-order velocity goes to 1, and equation (11) shows that the asymptotic thickness of the jet must also be 1. It follows from these remarks that $Q_0 = 1$. Hence, the last expansion (9) becomes

$$\psi^{(2)} = -1 + \epsilon\psi_1^{(2)} + \ldots \tag{17}$$

Representation in potential and hodograph planes. - Now the boundary value problem posed by the boundary conditions (14) to (16) is a simple free streamline problem which can be readily solved by the Helmholtz-Kirchhoff technique. The procedure for obtaining the solution is (ref. 2) to draw the region of flow in the hodograph plane and in the complex potential plane, and then to find the appropriate mapping of these two planes into some convenient intermediate plane (say, the T-plane). The shapes of these regions can readily be deduced from the boundary conditions (14) to (16), and they are shown in figures 3 and 4. (We have put $w_0 = \varphi_0 + i\psi_0$ in fig. 3.) The corresponding points in the various planes are designated by the same numbers. The zeroth-order "slip lines" are shown dashed in these figures since they do not correspond to lines of discontinuity and therefore can be ignored as far as obtaining the zeroth-order solution is concerned.

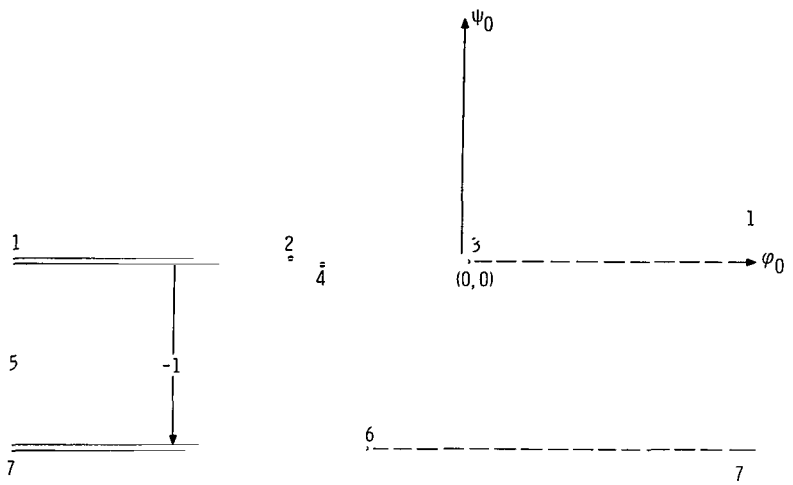

Figure 3. - Zeroth-order complex potential plane (w_0-plane).

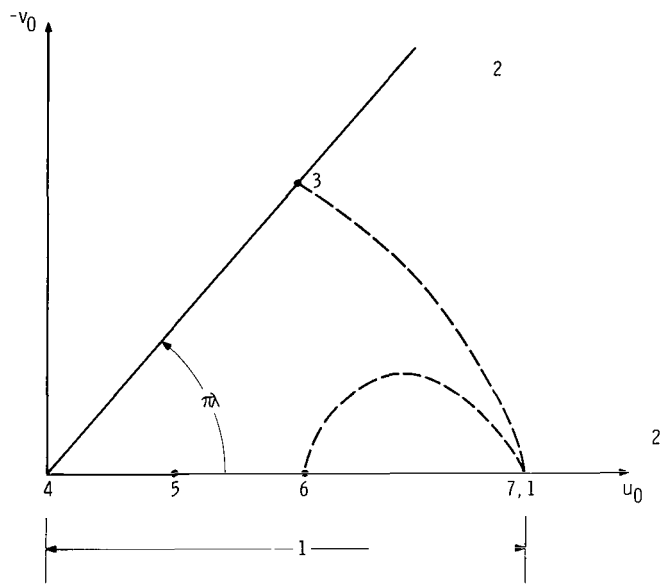

Figure 4. - Zeroth-order hodograph (ζ_0-plane).

Intermediate T-plane. - The intermediate T-plane is chosen in such a way that the region of flow maps into the upper half plane in the manner indicated in figure 5. We shall denote the real and imaginary parts of the variable T by ξ and η, respectively. The region of the T-plane into which the zeroth-order flow field interior to the jet maps is denoted by $\mathscr{D}^{I}$, and the region of the T-plane into which the zeroth-order main stream maps is denoted by $\mathscr{D}^{II}$. The dividing lines between these two regions corresponding to the slip lines $S_0^{(1)}$ and $S_0^{(2)}$ (which for convenience are called the zeroth-order slip lines

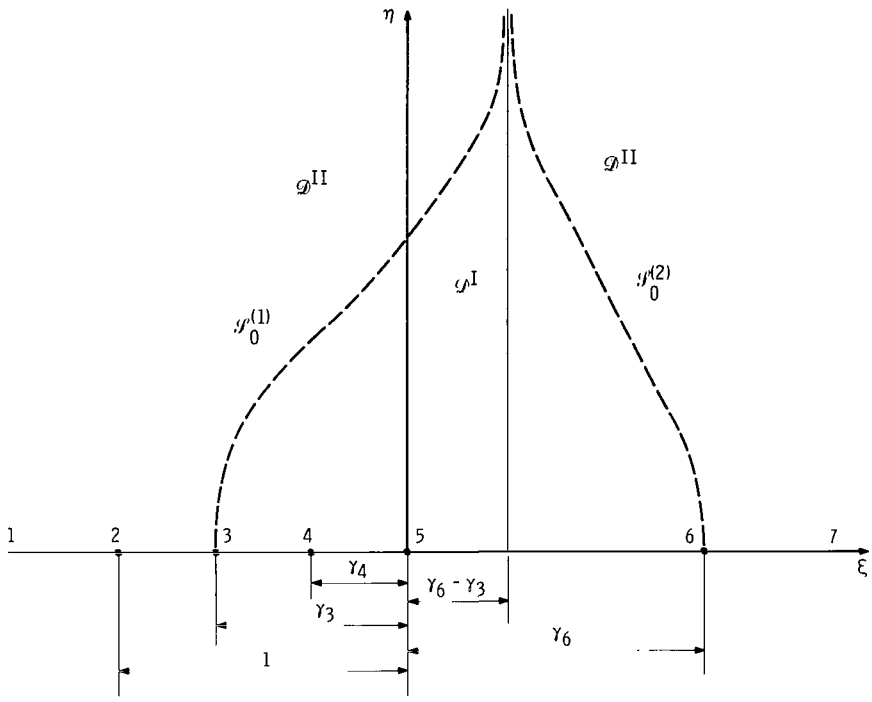

Figure 5. - Intermediate plane for $\gamma_6 > \gamma_3$ (T-plane).

even though no slip occurs in the zeroth-order solution) are denoted by $\mathcal{S}_0^{(1)}$ and $\mathcal{S}_0^{(2)}$, respectively. The figure is drawn for the case where $\gamma_6 > \gamma_3$. The situation where $\gamma_3 > \gamma_6$ can also occur. However, we show only the former case. In the latter case the two zeroth-order slip lines will approach each other asymptotically at the left of the imaginary axis. Otherwise the figures will look the same.

Mapping of potential and hodograph planes into intermediate T-plane. - A simple application of the Schwartz-Christoffel transformation (ref. 3) shows that the mapping which properly transforms the w_0-plane into the upper half T-plane in the manner indicated in the figures is defined by

$$\frac{dw_0}{dT} = -\frac{1}{\pi\gamma_3\gamma_6}\frac{(T + \gamma_3)(T - \gamma_6)}{T} \qquad \text{for } \eta \geq 0 \tag{18}$$

or, by performing the indicated integration,

$$w_0 = \frac{1}{\pi}\left[\ln\frac{T}{\gamma_3} - \frac{1}{2\gamma_3\gamma_6}\left(T^2 - \gamma_3^2\right) + \frac{(\gamma_6 - \gamma_3)}{\gamma_3\gamma_6}(T + \gamma_3)\right] - i \tag{19}$$

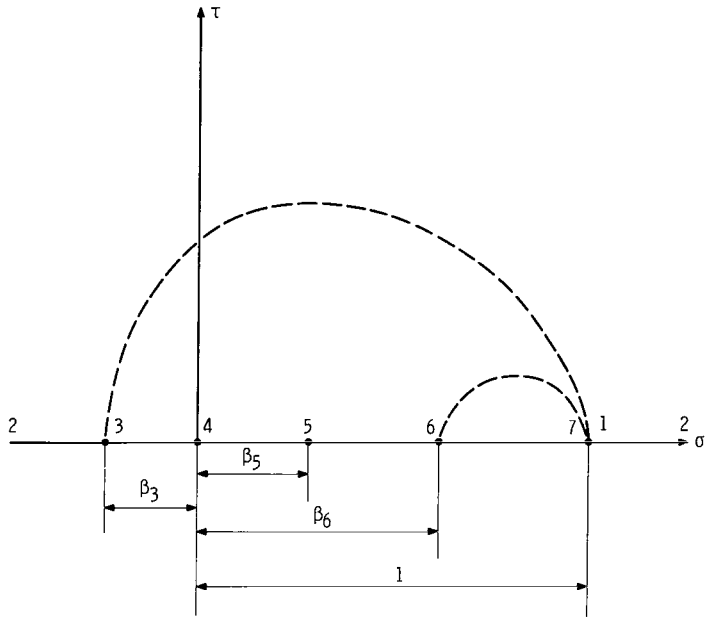

Figure 6. - Intermediate plane (Ω -plane).

The mapping of the zeroth-order hodograph plane (fig. 4) into the upper half T-plane is best accomplished by introducing the intermediate Ω-plane (with $\Omega = \sigma + i\tau$) shown in figure 6. The mapping that transforms the ζ_0 plane into the upper half Ω-plane in the manner indicated in the figures is

$$\zeta_0 = \Omega^{\lambda} \qquad \text{for} \quad \tau \geq 0 \tag{20}$$

On the other hand, the linear fractional transform

$$\Omega = \frac{T + \gamma_4}{T + 1} \qquad \text{for} \quad \eta \geq 0 \tag{21}$$

transforms the upper half T-plane into the upper half Ω-plane in the manner indicated in the figures. The relation between the γ's and β's is

$$\left.\begin{aligned} \beta_3 &= \frac{\gamma_3 - \gamma_4}{1 - \gamma_3} \\ \beta_5 &= \gamma_4 \\ \beta_6 &= \frac{\gamma_6 + \gamma_4}{\gamma_6 + 1} \end{aligned}\right\} \tag{22}$$

Equations (20) and (21) can now be combined to show that the mapping of the upper half T-plane into the ζ_0-plane is

$$\zeta_0 = \left(\frac{T + \gamma_4}{T + 1}\right)^{\lambda} \quad \text{for} \quad \eta \geq 0 \tag{23}$$

Relation of mapped coordinates to physical dimensions. - It is necessary to relate the γ's, or equivalently the β's, to the physical parameters involved in the problem. This is most conveniently done by working in the Ω-plane. In order to do this, however, it is first necessary to obtain $dw_0/d\Omega$ as a function of Ω. To this end notice that equation (21) can be solved for T to obtain

$$T = \frac{\gamma_4 - \Omega}{\Omega - 1} \tag{24}$$

Hence,

$$\frac{dT}{d\Omega} = \frac{1 - \gamma_4}{(\Omega - 1)^2} \tag{25}$$

Evidently,

$$\frac{dw_0}{d\Omega} = \frac{dw_0}{dT}\frac{dT}{d\Omega} \tag{26}$$

Substituting in equations (18), (22), (24), and (25) shows that

$$\frac{dw_0}{d\Omega} = \frac{(1 - \gamma_4)(1 - \gamma_3)(1 + \gamma_6)}{\pi\gamma_3\gamma_6} \frac{(\Omega + \beta_3)(\Omega - \beta_6)}{(\Omega - \beta_5)(\Omega - 1)^3} \tag{27}$$

But equations (22) can be solved for the γ's in terms of the β's to obtain

$$\left.\begin{aligned} \gamma_3 &= \frac{\beta_3 + \beta_5}{1 + \beta_3} \\ \gamma_4 &= \beta_5 \\ \gamma_6 &= \frac{\beta_6 - \beta_5}{1 - \beta_6} \end{aligned}\right\} \tag{28}$$

Substituting these into equation (27) gives

$$\frac{dw_0}{d\Omega} = \frac{(\beta_5 - 1)^3}{\pi(\beta_3 + \beta_5)(\beta_5 - \beta_6)} \frac{(\Omega + \beta_3)(\Omega - \beta_6)}{(\Omega - \beta_5)(\Omega - 1)^3} \tag{29}$$

But the first equation (10) shows that

$$\frac{dz}{d\Omega} = \frac{dz}{dw_0} \frac{dw_0}{d\Omega} = \frac{1}{\zeta_0} \frac{dw_0}{d\Omega}$$

Hence, it follows from equations (20) and (29) that

$$z = \int \frac{dz}{d\Omega} d\Omega = \frac{(\beta_5 - 1)^3}{\pi(\beta_3 + \beta_5)(\beta_5 - \beta_6)} \int \frac{1}{\Omega^\lambda} \frac{(\Omega + \beta_3)(\Omega - \beta_6)}{(\Omega - \beta_5)(\Omega - 1)^3} d\Omega \tag{30}$$

The integral can now be used to relate the various lengths in the physical plane (fig. 2) to the γ's and/or the β's.

Thus, it can be seen from figure 2(b) that the length l is given by the absolute value of the integral carried out between points 3 and 4. Or upon deforming the contour to lie along the real axis in the Ω-plane,

$$l = \left| \frac{(1 - \beta_5)^3}{\pi(\beta_3 + \beta_5)(\beta_6 - \beta_5)} \int_{-\beta_3}^{0} \frac{1}{(\sigma)^\lambda} \frac{(\sigma + \beta_3)(\sigma - \beta_6)}{(\sigma - \beta_5)(\sigma - 1)^3} d\sigma \right|$$

Upon changing the variable of integration from σ to $-\sigma$ this becomes

$$l = \frac{(1 - \beta_5)^3}{\pi(\beta_3 + \beta_5)(\beta_6 - \beta_5)} \int_{0}^{\beta_3} \frac{1}{\sigma^\lambda} \frac{(\beta_3 - \sigma)(\sigma + \beta_6)}{(\sigma + 1)^3(\sigma + \beta_5)} d\sigma \tag{31}$$

On the other hand, in order that the points 2 and 4 correspond to the same point in the physical plane, we see from equation (30) that we must have

$$0 = \int_{-\infty}^{0} \frac{1}{(-\sigma)^\lambda} \frac{(\sigma + \beta_3)(\sigma - \beta_6)}{(\sigma - \beta_5)(\sigma - 1)^3} d\sigma$$

Expanding the integrand in partial fractions gives

$$\int_{-\infty}^{0} \frac{1}{(-\sigma)^\lambda} \frac{d\sigma}{\sigma - \beta_5} - \int_{-\infty}^{0} \frac{1}{(-\sigma)^\lambda} \frac{d\sigma}{\sigma - 1} - (\beta_5 - 1) \int_{-\infty}^{0} \frac{1}{(-\sigma)^\lambda} \frac{d\sigma}{(\sigma - 1)^2}$$

$$+ \frac{(\beta_5 - 1)^3}{(\beta_3 + \beta_5)(\beta_5 - \beta_6)} \left[\int_{-\infty}^{0} \frac{1}{(-\sigma)^\lambda} \frac{d\sigma}{(\sigma - 1)^2} + \frac{(\beta_6 - 1)(\beta_3 + 1)}{(\beta_5 - 1)} \int_{-\infty}^{0} \frac{1}{(-\sigma)^\lambda} \frac{d\sigma}{(\sigma - 1)^3} \right] = 0$$

By changing the variable of integration from σ to $-\sigma/\beta_5$ in the first integral, and from σ to $-\sigma$ in the remaining integrals, each of these integrals becomes a beta-function. We, therefore, obtain

$$\left(1 - \frac{1}{\beta_5^{\lambda}}\right)B(1 - \lambda, \lambda) - (\beta_5 - 1)B(1 - \lambda, 1 + \lambda)$$

$$+ \frac{(\beta_5 - 1)^3}{(\beta_3 + \beta_5)(\beta_5 - \beta_6)}\left[B(1 - \lambda, 1 + \lambda) - \frac{(\beta_6 - 1)(\beta_3 + 1)}{\beta_5 - 1} B(1 - \lambda, 2 + \lambda)\right] = 0$$

Because $B(m, n) = \Gamma(m)\Gamma(n)/\Gamma(m + n)$ where Γ is the gamma-function, this becomes

$$\left(1 - \frac{1}{\beta_5^{\lambda}}\right)\frac{\Gamma(1 - \lambda)\Gamma(\lambda)}{\Gamma(1)} - (\beta_5 - 1)\frac{\Gamma(1 - \lambda)\Gamma(1 + \lambda)}{\Gamma(2)}$$

$$+ \frac{(\beta_5 - 1)^3}{(\beta_3 + \beta_5)(\beta_5 - \beta_6)}\left[\frac{\Gamma(1 - \lambda)\Gamma(1 + \lambda)}{\Gamma(2)} - \frac{(\beta_6 - 1)(\beta_3 + 1)}{(\beta_5 - 1)}\frac{\Gamma(1 - \lambda)\Gamma(2 + \lambda)}{\Gamma(3)}\right] = 0$$

Using the properties of the gamma-function to simplify we get, upon dividing through by $\Gamma(\lambda)$ and $\Gamma(1 - \lambda)$ and rearranging

$$(\beta_5 - \beta_6)(\beta_5 + \beta_3)\left[1 - \frac{1}{\beta_5^{\lambda}} - \lambda(\beta_5 - 1)\right] = \frac{\lambda(\lambda + 1)}{2}(\beta_5 - 1)^2(\beta_3 + 1)(\beta_6 - 1) - \lambda(\beta_5 - 1)^3 \qquad (32)$$

Finally, it can be seen from figure 2(b) that carrying out the integral (30) from point 4 to point 6 yields $-(r + ih)$. Hence, upon deforming the contour of integration to

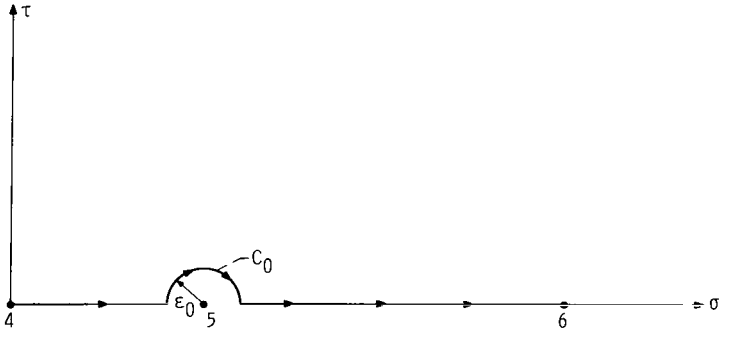

Figure 7. - Path of integration in Ω-plane.

the path shown in figure 7 we get in the limit as $\epsilon_0 \to 0$

$$-(r + ih) = \frac{(1 - \beta_5)^3}{\pi(\beta_3 + \beta_5)(\beta_6 - \beta_5)} \mathscr{P}.\mathscr{V}. \int_0^{\beta_6} \frac{1}{\sigma^\lambda} \frac{(\beta_3 + \sigma)(\beta_6 - \sigma)}{(\sigma - \beta_5)(1 - \sigma)^3} d\sigma$$

$$+ \lim_{\epsilon_0 \to 0} \frac{(\beta_5 - 1)^3}{\pi(\beta_3 + \beta_5)(\beta_5 - \beta_6)} \oint_{C_0} \frac{1}{\Omega^\lambda} \frac{(\Omega + \beta_3)(\Omega - \beta_6)}{(\Omega - \beta_5)(\Omega - 1)^3} d\Omega$$

where $\mathscr{P}.\mathscr{V}.$ denotes that the Cauchy principle value is to be taken. Hence, equating real and imaginary parts gives

$$r = \frac{(1 - \beta_5)^3}{\pi(\beta_3 + \beta_5)(\beta_6 - \beta_5)} \mathscr{P}.\mathscr{V}. \int_0^{\beta_6} \frac{1}{\sigma^\lambda} \frac{(\beta_3 + \sigma)(\sigma - \beta_6)}{(\sigma - \beta_5)(1 - \sigma)^3} d\sigma \tag{33}$$

and

$$-ih = \lim_{\epsilon_0 \to 0} \frac{(\beta_5 - 1)^3}{\pi(\beta_3 + \beta_5)(\beta_5 - \beta_6)} \oint_{C_0} \frac{1}{\Omega^\lambda} \frac{(\Omega + \beta_3)(\Omega - \beta_6)}{(\Omega - \beta_5)(\Omega - 1)^3} d\Omega$$

$$= \lim_{\epsilon_0 \to 0} \frac{1}{\pi\beta_5^\lambda} \oint_{C_0} \frac{d\Omega}{\Omega - \beta_5} = \frac{1}{\pi\beta_5^\lambda} \lim_{\epsilon_0 \to 0} \left[\ln(\Omega - \beta_5) \Big|_{\Omega = \beta_5 + \epsilon_0 e^{i0}}^{\Omega = \beta_5 + \epsilon_0 e^{i\pi}} \right]$$

$$= \frac{1}{\pi\beta_5^\lambda} \lim_{\epsilon_0 \to 0} [\ln \xi - \ln \xi - i\pi] = -\frac{i}{\beta_5^\lambda}$$

Hence,

$$h = \frac{1}{\beta_5^{\lambda}} \tag{34}$$

Thus, equations (31), (32), and (33) serve to determine β_3, β_5, and β_6 in terms of the lengths l and r; and equation (34) gives the ratio of nozzle width to zeroth-order asymptotic jet width h in terms of β_5 and λ. The constants γ_3, γ_4, and γ_6 can be determined from equation (28) once the β's are found.

Equations of zeroth-order slip lines in intermediate T-plane. - To obtain the first-order solution it is necessary to first find the equations of the zeroth-order slip lines in the T-plane, $\mathcal{S}_0^{(1)}$ and $\mathcal{S}_0^{(2)}$. To this end, note that figures 3 and 5 show that

$$\mathcal{Im}\, w_0(T) = 0 \qquad \text{whenever} \quad T \in \mathcal{S}_0^{(1)}$$

and

$$\mathcal{Im}\, w_0(T) = -1 \qquad \text{whenever} \quad T \in \mathcal{S}_0^{(2)}$$

Upon introducing polar coordinates into the T-plane

$$T = \rho e^{i\theta} \tag{35}$$

equation (19) shows that

$$w_0(T) = \frac{1}{\pi}\left[\ln\frac{\rho}{\gamma_3} - \frac{\rho^2\cos 2\theta - \gamma_3^2}{2\gamma_3\gamma_6} - \frac{\gamma_3 - \gamma_6}{\gamma_3\gamma_6}(\rho\cos\theta + \gamma_3)\right]$$

$$+ \frac{i}{\pi}\left[\theta - \pi - \frac{1}{2\gamma_3\gamma_6}\rho^2\sin 2\theta - \frac{\gamma_3 - \gamma_6}{\gamma_3\gamma_6}\rho\sin\theta\right] \qquad 0 \le \theta \le \pi$$

Setting the imaginary part of this expression to zero and to -1 we find that

$$\gamma_3\gamma_6(\pi - \theta) + \frac{1}{2}\rho^2\sin 2\theta + (\gamma_3 - \gamma_6)\rho\sin\theta = 0 \qquad \text{for} \quad T \in \mathcal{S}_0^{(1)} \tag{36}$$

and

$$-\gamma_3\gamma_6\theta + \frac{1}{2}\rho^2 \sin 2\theta + (\gamma_3 - \gamma_6)\rho \sin\theta = 0 \qquad \text{for } T \in \mathcal{S}_0^{(2)} \tag{37}$$

Each of these equations has three solutions. The solution $\theta = \pi$, $0 \le \rho < \infty$ of equation (36) and the solution $\theta = 0$, $0 \le \rho \le \infty$ of equation (37) are of no interest to us since they correspond to the solid boundaries which are mapped into the real axis in the T-plane. The remaining solutions to equations (36) and (37) are, respectively,

$$\rho = \frac{\gamma_6 - \gamma_3 \pm \sqrt{(\gamma_6 - \gamma_3)^2 + 4\gamma_3\gamma_6(\theta - \pi)\cot\theta}}{2\cos\theta} \qquad \theta_1 \le \theta < \pi \qquad \text{for } T \in \mathcal{S}_0^{(1)}$$

$$\rho = \frac{\gamma_6 - \gamma_3 \pm \sqrt{(\gamma_6 - \gamma_3)^2 + 4\gamma_3\gamma_6\theta\cot\theta}}{2\cos\theta} \qquad 0 < \theta \le \theta_2 \qquad \text{for } T \in \mathcal{S}_0^{(2)}$$

where (since ρ cannot be imaginary and, hence, the quantities under the square root signs must be positive) θ_1 and θ_2 are the solutions of the transcendental equations

$$\left.\begin{aligned} \tan\theta_1(\gamma_6 - \gamma_3)^2 + 4\gamma_3\gamma_6(\theta_1 - \pi) = 0 \qquad \text{for } \theta_1 > 0 \\ \tan\theta_2(\gamma_6 - \gamma_3)^2 + 4\gamma_3\gamma_6\theta_2 = 0 \qquad \text{for } \theta_2 > 0 \end{aligned}\right\} \tag{38}$$

and we have used the trigonometric identity $\sin 2\theta = 2 \sin\theta \cos\theta$. The proper choice of the + or - sign in front of the square root will be discussed subsequently. Hence, in view of equation (35) we can write

$$T = \frac{1}{2}\left[\gamma_6 - \gamma_3 \pm \sqrt{(\gamma_6 - \gamma_3)^2 + 4\gamma_3\gamma_6(\theta - \pi)\cot\theta}\right](1 + i\tan\theta)$$

$$\text{with } \theta_1 \le \theta < \pi \qquad \text{for } T \in \mathcal{S}_0^{(1)} \tag{39}$$

$$T = \frac{1}{2}\left[\gamma_6 - \gamma_3 \pm \sqrt{\left(\gamma_6 - \gamma_3\right)^2 + 4\gamma_3\gamma_6\theta \cot \theta}\right](1 + i \tan \theta)$$

$$\text{with } 0 < \theta \leq \theta_2 \quad \text{for } T \in \mathscr{S}_0^{(2)} \tag{40}$$

When the proper signs are chosen, equations (39) and (40) are parametric equations for the zeroth-order slip lines with parameter θ. It is convenient to introduce a new parametric variable ω:

$$\omega = \begin{cases} \theta & \text{for } T \in \mathscr{S}_0^{(2)} \\ \theta - \pi & \text{for } T \in \mathscr{S}_0^{(1)} \end{cases}$$

Then in view of equation (38), equations (39) and (40) can be written as

$$T = T^{\pm}(\omega) \quad \text{with } -\omega_m \leq \omega < 0 \quad \text{for } T \in \mathscr{S}_0^{(1)} \tag{41}$$

$$T = T^{\pm}(\omega) \quad \text{with } 0 < \omega \leq \omega_m \quad \text{for } T \in \mathscr{S}_0^{(2)} \tag{42}$$

where we have put

$$T^{\pm}(\omega) \equiv \frac{1}{2}\left[\gamma_6 - \gamma_3 \pm \sqrt{\left(\gamma_6 - \gamma_3\right)^2 + 4\gamma_3\gamma_6\omega \cot \omega}\right](1 + i \tan \omega) \quad \text{for } -\omega_m \leq \omega \leq \omega_m \tag{43}$$

and ω_m is the solution of the transcendental equation

$$\left(\gamma_6 - \gamma_3\right)^2 \tan \omega_m + 4\gamma_3\gamma_6\omega_m = 0 \quad \text{for } \omega_m \geq 0 \tag{44}$$

Note that the solutions of this equation will always be such that $\omega_m > \pi/2$. The ω_m corresponds to the location along a slip line where $d\theta/dp = 0$ (see fig. 8). In order to completely determine the parametric equations of $\mathscr{S}_0^{(1)}$ and $\mathscr{S}_0^{(2)}$, we must determine when the + and - signs hold in equations (41) and (42). First note that

$$T^{+}(0) = \gamma_6 \tag{45}$$

and

$$T^{-}(0) = -\gamma_3 \tag{46}$$

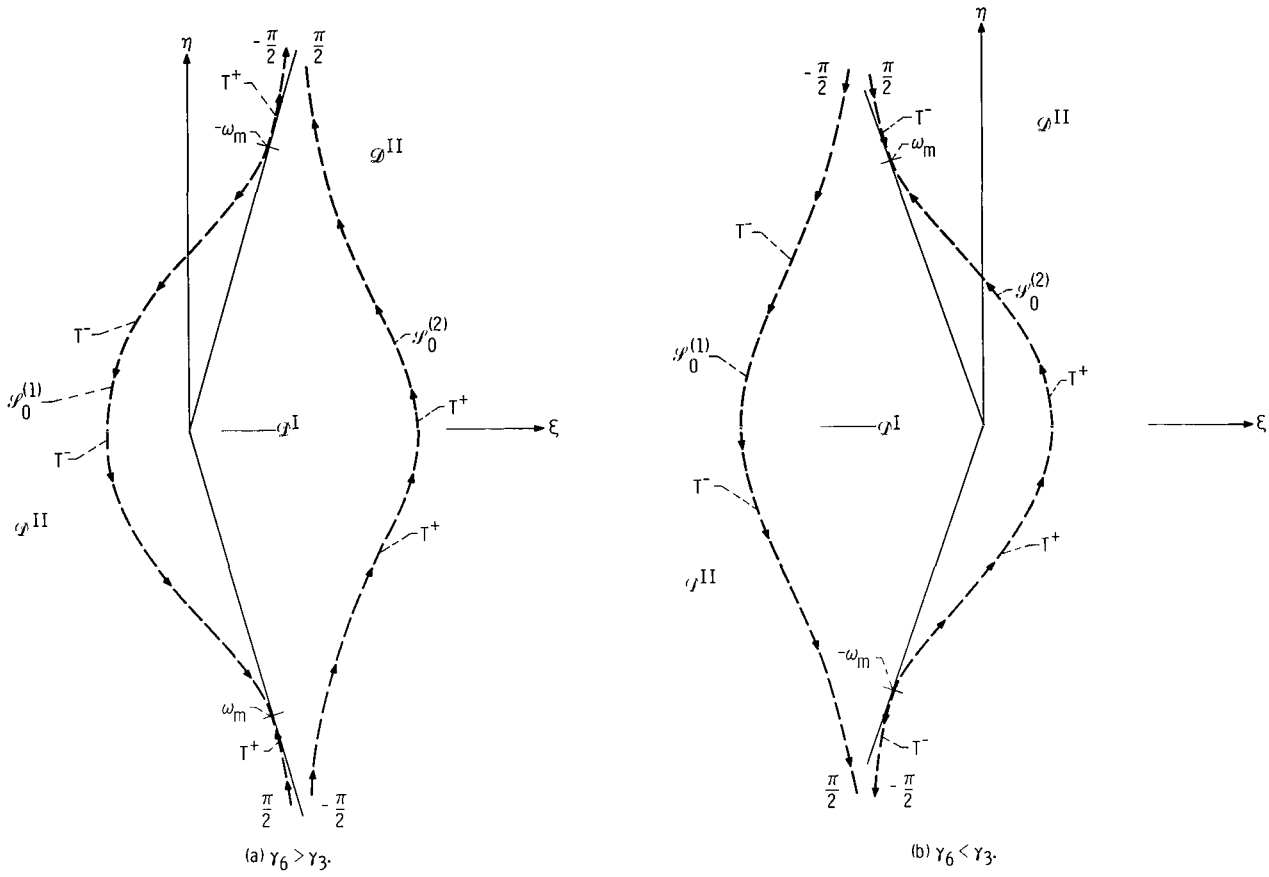

(a) $\gamma_6 > \gamma_3$.

(b) $\gamma_6 < \gamma_3$.

Figure 8. - Extended T-plane.

In order to proceed further we must consider the two cases $\gamma_6 > \gamma_3$ and $\gamma_6 < \gamma_3$ separately. First consider the case where $\gamma_6 > \gamma_3$. This corresponds to the situation depicted in figure 5. Note that the conditions (45) and (46) show (see fig. 5) that we must have

$$T = T^+(\omega) \quad \text{for} \quad T \in \mathcal{S}_0^{(2)}$$

$$T = T^-(\omega) \quad \text{for} \quad T \in \mathcal{S}_0^{(1)}$$

when ω is near zero. Now for $\gamma_6 > \gamma_3$ we will have

$$T^+(\omega) \to \infty \quad \text{as} \quad \omega \to \frac{\pi}{2} < \omega_m$$

Hence, $T^+(\omega)$ will transverse the entire contour $\mathcal{S}^{(2)}$ in a counterclockwise direction as

ω varies from zero to $\pi/2$. On the other hand, $T^-(\omega)$ will remain finite when $\omega = -\pi/2$, and the curve $\mathscr{C}^{(1)}$ will cross the imaginary axes when this occurs. In fact, it will remain finite even when $\omega = -\omega_m$, at which point T^+ and T^- become equal. In order to obtain the remaining portion of $\mathscr{C}^{(1)}$, we must take

$$T = T^+(\omega) \qquad \text{with} \quad -\omega_m \leq \omega < -\frac{\pi}{2}$$

for this will continue $\mathscr{C}_0^{(1)}$ smoothly from $T^-(-\omega_m)$ to infinity.

Hence, we have

$$T = \left.\begin{cases} \left.\begin{cases} T^-(\omega) & \text{with } -\omega_m \leq \omega < 0 \text{ for } |T| \leq \rho_m \\ T^+(\omega) & \text{with } -\omega_m \leq \omega_m < -\frac{\pi}{2} \text{ for } |T| \geq \rho_m \end{cases}\right\} \text{for } T \in \mathscr{C}_0^{(1)} \\ T = T^+(\omega) \quad \text{with } 0 < \omega < \frac{\pi}{2} \quad \text{for } T \in \mathscr{C}_0^{(2)} \end{cases}\right\} \text{for } \gamma_6 > \gamma_3 \qquad (47)$$

where we have put

$$\rho_m \equiv \left|\frac{\gamma_6 - \gamma_3}{2}\right| \sqrt{1 + \tan^2 \omega_m}$$

Note that the curve $\mathscr{C}^{(2)}$ is traversed in a counterclockwise direction when ω is increasing and that the curve $\mathscr{C}^{(1)}$ is traversed in a counterclockwise direction with ω increasing for $|T| > \rho_m$.

Precisely the same type of reasoning now shows that

$$\left.\begin{cases} T = T^-(\omega) \quad \text{with } -\frac{\pi}{2} < \omega < 0 \text{ for } T \in \mathscr{C}_0^{(1)} \\ T = \left\{\begin{array}{ll} T^+(\omega) & \text{with } 0 < \omega \leq \omega_m \text{ for } |T| \leq \rho_m \\ T^-(\omega) & \text{with } \frac{\pi}{2} < \omega \leq \omega_m \text{ for } |T| \geq \rho_m \end{array}\right. \text{for } T \in \mathscr{C}_0^{(2)} \end{cases}\right\} \text{for } \gamma_6 < \gamma_3 \qquad (48)$$

Relation between points in physical and intermediate T-planes. - It follows from the first equation (10) that the points in the physical plane (fig. 2(b)) are related to the points in the T-plane by

$$z(T) = \int \frac{1}{\zeta_0(T)} \frac{dw_0}{dT} dT + \text{constant} \tag{49}$$

Substituting equations (18) and (23) in this formula and using the fact, indicated in figure 2(b), that the origin of the coordinate system in the physical plane is to be at the point 2 result in

$$z(T) = -\frac{1}{\pi\gamma_3\gamma_6} \int_{-1}^{T} \left(\frac{T+1}{T+\gamma_4}\right)^{\lambda} \frac{(T+\gamma_3)(T-\gamma_6)}{T} dT \tag{50}$$

Formulation of First-Order Problem in Physical Plane

The mapping $T \rightarrow z$ defined by equation (50) transforms the upper half T-plane approximately into the region of flow in the physical plane. The domain $\mathscr{D}^I$ is mapped into the shaded region of the physical plane shown in figure 9. The curves $\mathscr{S}_0^{(1)}$ and $\mathscr{S}_0^{(2)}$ are mapped into the dashed boundaries $S_0^{(1)}$ and $S_0^{(2)}$, respectively, of this region. This region, of course, differs from the true interior of the jet whose boundaries $S^{(1)}$ and $S^{(2)}$ are indicated by the solid (curved) lines in figure 9.

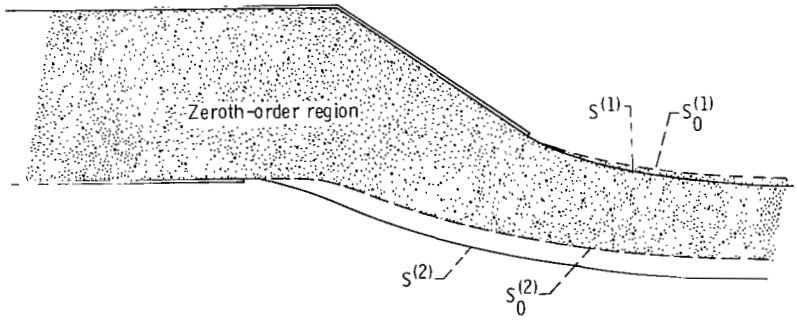

Figure 9. - Comparison of zeroth-order and true jet boundaries in physical plane.

Relation between quantities on unknown slip lines to quantities on known zeroth-order slip lines. - Now the first two groups of boundary conditions in equation (8) are specified on the curves $S^{(1)}$ and $S^{(2)}$ in the physical plane, whose shapes are not known at this stage of the solution. As explained in reference 1, however, these boundary conditions, correct to terms of order ϵ, can be transferred to $S_0^{(1)}$ and $S_0^{(2)}$ by relating the values of ζ^I, ζ^{II}, w^I, and w^{II} at an arbitrary point $z^{(1)}$ of $S^{(1)}$ or an arbitrary point $z^{(2)}$ of $S^{(2)}$ to their values at some neighboring point $z_0^{(1)}$ of $S_0^{(1)}$ or $z_0^{(2)}$ of $S_0^{(2)}$, respectively, by performing a Taylor series expansion of these quantities about $z_0^{(1)}$ or $z_0^{(2)}$. Thus,

$$\zeta^{\nu}\left(z^{(j)}\right) = \zeta^{\nu}\left(z_0^{(j)}\right) + \left(\frac{d\zeta^{\nu}}{dz}\right)_{z=z_0^{(j)}} \left(z^{(j)} - z_0^{(j)}\right) + \ldots \qquad \text{for } \nu = I, II;\ j = 1, 2$$

$$w^{\nu}\left(z^{(j)}\right) = w^{\nu}\left(z_0^{(j)}\right) + \zeta^{\nu}\left(z_0^{(j)}\right)\left(z^{(j)} - z_0^{(j)}\right) + \ldots \qquad \text{for } \nu = I, II;\ j = 1, 2$$

where the second and third equations (10) have been used.

Substituting the asymptotic expansions given by equation (9) into these Taylor series and neglecting terms of $O(\epsilon^3)$ yields

$$\zeta^{\nu}\left(z^{(j)}\right) = \zeta_0\left(z_0^{(j)}\right) + \epsilon\left[\zeta_1^{\nu}\left(z_0^{(j)}\right) + \left(\frac{d\zeta_0}{dz}\right)_{z=z_0^{(j)}} z_1^{(j)}\right] + O(\epsilon^2) \qquad \text{for } \nu = I, II;\ j = 1, 2 \tag{51}$$

$$w^{\nu}\left(z^{(j)}\right) = w_0\left(z_0^{(j)}\right) + \epsilon\left[w_1^{\nu}\left(z_0^{(j)}\right) + \zeta_0\left(z_0^{(j)}\right) z_1^{(j)}\right] + O(\epsilon^2) \qquad \text{for } \nu = I, II;\ j = 1, 2 \tag{52}$$

These expressions relate the values of the dependent variables w^I, w^{II}, ζ^I, and ζ^{II} at the points of the unknown boundaries $S^{(1)}$ and $S^{(2)}$ to their values on the known boundaries $S_0^{(1)}$ and $S_0^{(2)}$, respectively, with an error of order ϵ^2. It can now be shown from equation (51) that

$$\left|\zeta^{\nu}\left(z^{(j)}\right)\right|^2 = \left|\zeta_0\left(z_0^{(j)}\right)\right|^2$$

$$+ 2\epsilon\left|\zeta_0\left(z_0^{(j)}\right)\right|^2 Re\left[\frac{\zeta_1^{\nu}\left(z_0^{(j)}\right)}{\zeta_0\left(z_0^{(j)}\right)} + \frac{1}{\zeta_0\left(z_0^{(j)}\right)}\left(\frac{d\zeta_0}{dz}\right)_{z=z_0^{(j)}} z_1^{(j)}\right] + O(\epsilon^2) \qquad \text{for } \nu = I, II;\ j = 1, 2 \tag{53}$$

Boundary conditions along slip lines. - Substituting the expansions (17), (52), and (53) into the first two groups of boundary conditions in equation (8) and equating to zero the coefficients of ϵ to the first power yields the following first-order boundary conditions along the slip lines:

$$Re\left[\frac{\zeta^{I}\left(z_0^{(j)}\right)}{\zeta_0\left(z_0^{(j)}\right)} - \frac{\zeta^{II}\left(z_0^{(j)}\right)}{\zeta_0\left(z_0^{(j)}\right)}\right] = \frac{1}{2}\frac{1}{\left|\zeta_0\left(z_0^{(j)}\right)\right|^2} \qquad \text{for } j = 1,2 \tag{54}$$

$$Im\left[w_1^{\nu}\left(z_0^{(1)}\right) + \zeta_0\left(z_0^{(1)}\right)z_1^{(1)}\right] = 0 \qquad \text{for } \nu = I, II \tag{55}$$

$$Im\left[w_1^{\nu}\left(z_0^{(2)}\right) + \zeta_0\left(z_0^{(2)}\right)z_1^{(2)}\right] = \psi_1^{(2)} \qquad \text{for } \nu = I, II \tag{56}$$

Thus, equations (54) to (56) are the boundary conditions for the first-order solutions on the boundaries $S^{(1)}$ and $S^{(2)}$ "transferred" to the zeroth-order boundaries $S_0^{(1)}$ and $S_0^{(2)}$, respectively. Hence, the first-order boundary value problem has been transferred from one in which the shape of the boundaries is unknown to one in which it is known. Note, however, that these boundary conditions involve the variables w_1^{I}, w_1^{II}, ζ_1^{I}, ζ_1^{II}, $z_1^{(1)}$, and $z_1^{(2)}$. But ζ_1^{I} and ζ_1^{II} are completely determined in terms of w_1^{I} and w_1^{II}, respectively, by the second two equations (10). In view of this, equations (54) to (56) may be thought of as two boundary conditions connecting the variable ζ_1^{I} with the variable ζ_1^{II} across $S_0^{(1)}$ and $S_0^{(2)}$ (or equivalently the variable w^{I} with the variable w^{II}) plus two equations which determine $z_1^{(1)}$ and $z_1^{(2)}$ once ζ_1^{I} is known. Thus, it follows from equations (55) and (56)

$$Im\, w_1^{I}\left(z_0^{(j)}\right) = Im\, w_1^{II}\left(z_0^{(j)}\right) \qquad \text{for } j = 1,2 \tag{57}$$

Hence, in view of the second two equations (10), equations (54) and (57) are boundary conditions on $S_0^{(1)}$ and $S_0^{(2)}$ which connect the solution ζ_1^{I} in D^{I} with the solution ζ_1^{II} in D^{II}. And equations (55) and (56) with $\nu = I$ serve to determine $z_1^{(1)}$ and $z_1^{(2)}$, respectively, once ζ_1^{I} is known. (Actually, $z_1^{(1)}$ and $z_1^{(2)}$ will be determined in a slightly different fashion.) The conditions (57) can be differentiated with respect to w_0 along the zeroth-order slip lines to obtain, upon using the second and third equations (10),

$$Im\left[\frac{\zeta_1^{I}\left(z_0^{(j)}\right)}{\zeta_0\left(z_0^{(j)}\right)} - \frac{\zeta_1^{II}\left(z_0^{(j)}\right)}{\zeta_0\left(z_0^{(j)}\right)}\right] = 0 \qquad \text{for } j = 1,2$$

Multiplying this by i and adding it to equation (54) yields the following complex jump conditions along $S_0^{(1)}$ and $S_0^{(2)}$

$$\frac{\zeta^{I}\left(z_0^{(j)}\right)}{\zeta_0\left(z_0^{(j)}\right)} - \frac{\zeta^{II}\left(z_0^{(j)}\right)}{\zeta_0\left(z_0^{(j)}\right)} = \frac{1}{2\left|\zeta_0\left(z_0^{(j)}\right)\right|^2} \qquad \text{for } j = 1,2 \tag{58}$$

Boundary conditions along solid boundaries. - The boundary conditions for the remaining (solid) boundaries are easily deduced by substituting the first two asymptotic expansions in equation (9) into the boundary conditions (7) and (8) to obtain

$$\left.\begin{aligned} &\mathcal{Im}\ \zeta_1^{I}(z) = 0 \quad \text{for } z \in \widehat{45} \text{ and } z \in 56 \\ &\mathcal{Im}\ \zeta_1^{II}(z) = 0 \quad \text{for } z \in \widehat{12} \text{ and } z \in \widehat{67} \\ &\arg \zeta_1^{I}(z) = \pi\lambda \quad \text{for } z \in \widehat{34} \\ &\arg \zeta_1^{II}(z) = \pi\lambda \quad \text{for } z \in \widehat{23} \end{aligned}\right\} \tag{59}$$

$$\zeta_1^{II}(z) \to 0 \quad \text{for } z \to \text{point 1 and } z \to \text{point 7} \tag{60}$$

The second boundary condition (59) can be combined with the zeroth-order boundary condition (16) to obtain

$$\mathcal{Im}\ \frac{\zeta_1^{I}(z)}{\zeta_0(z)} = 0 \quad \text{for } z \in \widehat{34}$$

$$\mathcal{Im}\ \frac{\zeta_1^{II}(z)}{\zeta_0(z)} = 0 \quad \text{for } z \in \widehat{23}$$

Similar remarks apply for the first boundary conditions (59) and (14). Thus, the boundary conditions (59) can be rewritten as

$$\mathcal{Im}\ \frac{\zeta_1^{I}(z)}{\zeta_0(z)} = 0 \quad \text{for } z \in \widehat{34},\ z \in \widehat{45}, \text{ and } z \in \widehat{56} \tag{61}$$

$$\mathcal{I}m \frac{\zeta_1^{II}(z)}{\zeta_0(z)} = 0 \quad \text{for } z \in \widehat{12},\ z \in \widehat{23},\ z \in \widehat{67} \tag{62}$$

and equations (17) and (60) can be combined to yield

$$\frac{\zeta_1^{II}(z)}{\zeta_0(z)} \to 0 \quad \text{for } z \to \text{point 1 and } z \to \text{point 7} \tag{63}$$

Solution of First-Order Boundary Value Problem

Boundary value problem in T-plane. - The boundary conditions (57) and (61) to (63) completely determine a boundary value problem (or more precisely, two boundary value problems connected along the curves $S_0^{(1)}$ and $S_0^{(2)}$) for a holomorphic function in the zeroth-order region of flow in the physical plane. Under the change of variable $z \to T$ defined by equation (50), this boundary value problem can be transformed into one in the upper half T-plane (fig. 5). The boundary conditions in the T-plane become

$$\left.\begin{aligned} &\frac{\zeta_1^{I}(T)}{\zeta_0(T)} - \frac{\zeta_1^{II}(T)}{\zeta_0(T)} = \frac{1}{2}\frac{1}{|\zeta_0(T)|^2} \quad \begin{cases} \text{for } T \in \mathcal{S}_0^{(1)} \\ \text{for } T \in \mathcal{S}_0^{(2)} \end{cases} \\ &\mathcal{I}m \frac{\zeta_1^{I}(\xi + i0)}{\zeta_0(\xi + i0)} = 0 \quad \text{for } -\gamma_3 \le \xi \le \gamma_6 \\ &\mathcal{I}m \frac{\zeta_1^{II}(\xi + i0)}{\zeta_0(\xi + i0)} = 0 \quad \text{for } \xi \le -\gamma_3 \text{ and } \xi \ge \gamma_6 \\ &\frac{\zeta_1^{II}(T)}{\zeta_0(T)} \to 0 \quad \text{for } T \to \infty \end{aligned}\right\} \tag{64}$$

Use of sectionally analytic function Θ. - Clearly, the domains of definition of ζ_1^I and ζ_1^{II} are $\mathcal{D}^I$ and $\mathcal{D}^{II}$, respectively. It is convenient to work with the sectionally analytic function Θ defined in the upper half T-plane in terms of ζ_1^I and ζ_1^{II} by

$$\Theta(T) = \begin{cases} \Theta^{I}(T) \equiv \dfrac{\zeta_1^{I}(T)}{\zeta_0(T)} - \dfrac{1}{2} & \text{for } T \in \mathscr{D}^{I} \\ \Theta^{II}(T) \equiv \dfrac{\zeta_1^{II}(T)}{\zeta_0(T)} & \text{for } T \in \mathscr{D}^{II} \end{cases} \tag{65}$$

It follows from the boundary conditions given in equation (64) that Θ must satisfy the boundary conditions

$$\Theta^{I}(T) - \Theta^{II}(T) = \mu(T) \qquad \begin{cases} \text{for } T \in \mathscr{S}_0^{(1)} \\ \text{for } T \in \mathscr{S}_0^{(2)} \end{cases} \tag{66}$$

$$\mathscr{Im}\, \Theta(\xi + i0) = 0 \qquad \text{for } -\infty < \xi < \infty \tag{67}$$

$$\Theta(T) \to 0 \qquad \text{for } T \to \infty \tag{68}$$

where we have put

$$\mu(T) \equiv \frac{1}{2}\left[\frac{1}{\left|\zeta_0(T)\right|^2} - 1\right] \tag{69}$$

Since ζ_1^{I} and ζ_1^{II} can be no more singular than ζ_0 if the asymptotic expansion is to be uniformly valid, it follows that Θ must be bounded in the entire upper half T-plane including the real axis.

Now the Schwarz reflection principle shows that the boundary condition (67) will be satisfied if, and only if, the function Θ is analytically continued into the lower half plane by the formula

$$\Theta(T) = \overline{\Theta(\overline{T})} \qquad \text{for } \eta \leq 0 \tag{70}$$

This can be done by first extending the curves $\mathscr{S}_0^{(1)}$ and $\mathscr{S}_0^{(2)}$ into the lower half plane in such a way that they are symmetric with respect to the ξ-axis as shown in figure 8. This extension can be accomplished algebraically simply by extending the range of the parametric variable ω so that it is symmetric with respect to the origin in the parametric equations (47) and (48) for the curves $\mathscr{S}_0^{(1)}$ and $\mathscr{S}_0^{(2)}$. Thus, the parametric equations of the extended curves $\mathscr{S}_0^{(1)}$ and $\mathscr{S}_0^{(2)}$ shown in figure 8 are

$$T = \left\{ \begin{array}{ll} T^-(\omega) & \text{with } -\omega_m \le \omega \le \omega_m \text{ for } |T| \le \rho_m \\ T^+(\omega) & \text{with } -\omega_m \le \omega < -\frac{\pi}{2} \text{ and } \frac{\pi}{2} < \omega \le \omega_m \text{ for } |T| \ge \rho_m \end{array} \right\} \text{ for } T \in \mathcal{S}_0^{(1)} \quad \left. \begin{array}{l} \\ \\ \\ \end{array} \right\} \text{ for } \gamma_6 > \gamma_3 \tag{71}$$

and

$$T = T^+(\omega) \quad \text{with } -\frac{\pi}{2} < \omega < \frac{\pi}{2} \text{ for } T \in \mathcal{S}_0^{(2)}$$

(71)

$$T = T^-(\omega) \quad \text{with } -\frac{\pi}{2} < \omega < \frac{\pi}{2} \text{ for } T \in \mathcal{S}_0^{(1)}$$

$$T = \left\{ \begin{array}{ll} T^+(\omega) & \text{with } -\omega_m \le \omega \le \omega_m \text{ for } |T| \le \rho_m \\ T^-(\omega) & \text{with } -\omega_m \le \omega < -\frac{\pi}{2} \text{ and } \frac{\pi}{2} < \omega \le \omega_m \text{ for } |T| \ge \rho_m \end{array} \right\} \text{ for } T \in \mathcal{S}_0^{(2)} \quad \left. \begin{array}{l} \\ \\ \\ \end{array} \right\} \text{ for } \gamma_6 < \gamma_3 \tag{72}$$

The arrows in figure 8 indicate the direction in which the curves are traversed with ω increasing.

Next it is necessary to extend the definition of the jump $\mu(T)$ to the negative half T-plane. It is clear that this jump must have the same symmetry properties as $\Theta(T)$ with respect to the real axis. Hence, we must have

$$\mu(T) = \overline{\mu(\overline{T})} \quad \text{for } \eta \le 0 \tag{73}$$

Substituting equation (23) into equation (69) shows that for $\eta \ge 0$

$$\mu(T) = \frac{1}{2}\left[\left(\frac{|T|^2 + 2\mathcal{R}e\,T + 1}{|T|^2 + 2\gamma_4 \mathcal{R}e\,T + \gamma_4^2}\right)^{\lambda} - 1\right] \tag{74}$$

But since

$$\overline{\left(\frac{|T|^2 + 2\mathcal{R}e\,\overline{T} + 1}{|T|^2 + 2\gamma_4 \mathcal{R}e\,\overline{T} + \gamma_4^2}\right)^{\lambda} - 1} = \left(\frac{|T|^2 + 2\mathcal{R}e\,T + 1}{|T|^2 + 2\gamma_4 \mathcal{R}e\,T + \gamma_4^2}\right)^{\lambda} - 1$$

we see that the symmetry conditions (73) will be satisfied if we take equation (74) as the definition of $\mu(T)$ in the negative half plane also. We now require that the jump condi-

tion (66) hold along the extended curves $\mathscr{S}_0^{(1)}$ and $\mathscr{S}_0^{(2)}$ with $\mu(T)$ defined in the entire T-plane by (74) and that equation (68) hold in the negative half plane also. Then the boundary condition (67) will be automatically satisfied (see ref. 4).

Determination of Θ by Cauchy integrals along slip lines. - Since $\mu(T) \to 0$ as $T \to \infty$, the sectionally analytic function Θ which satisfies the jump conditions (66) on the extended curves $\mathscr{S}_0^{(1)}$ and $\mathscr{S}_0^{(2)}$, which has the behavior given by equation (68) at $T = \infty$, and which is analytic at every other point of the T-plane can be represented by two Cauchy integrals as (ref. 4)

$$\Theta(T) = \frac{1}{2\pi i} \int_{\mathscr{S}_1} \frac{\mu(t)}{t - T}\, dt + \frac{1}{2\pi i} \int_{\mathscr{S}_2} \frac{\mu(t)}{t - T}\, dt \tag{75}$$

where the direction of integration is such that the region I is to the left when traversing the contour. In order to evaluate these integrals we must first transform them to integrals with respect to the parametric variable ω.

Since the variable of integration t traverses the contours $\mathscr{S}_0^{(1)}$ and $\mathscr{S}_0^{(2)}$, this change of variable is accomplished simply by substituting in the parametric representations (71) and (72) of the contours $\mathscr{S}_0^{(1)}$ and $\mathscr{S}_0^{(2)}$. When this is done and the directions of integration indicated in figure 8 are taken into account, we obtain

$$\Theta(T) = \frac{1}{2\pi i} \int_{-\omega_m}^{\omega_m} \frac{M^+(\omega)}{T^+(\omega) - T} \frac{dT^+(\omega)}{d\omega}\, d\omega + \frac{1}{2\pi i} \int_{-\omega_m}^{\omega_m} \frac{M^-(\omega)}{T^-(\omega) - T} \frac{dT^-(\omega)}{d\omega}\, d\omega \tag{76}$$

where we have defined $M^{\pm}(\omega)$ by

$$\left.\begin{aligned} M^+(\omega) &= \begin{cases} \mu(T^+(\omega)) & \text{for } |\omega| < \dfrac{\pi}{2} \\ -\mu(T^+(\omega)) & \text{for } \dfrac{\pi}{2} < |\omega| \le \omega_m \end{cases} \\ M^-(\omega) &= \mu(T^-(\omega)) \qquad \text{for } |\omega| \le \omega_m \end{aligned}\right\} \quad \text{for } \gamma_6 > \gamma_3$$

and

and

$$\left.\begin{aligned} M^{+}(\omega) &= \mu(T^{+}(\omega)) \quad \text{for} \quad |\omega| \le \omega_m \\ M^{-}(\omega) &= \begin{cases} \mu(T^{-}(\omega)) & \text{for} \quad |\omega| < \dfrac{\pi}{2} \\ -\mu(T^{-}(\omega)) & \text{for} \quad \dfrac{\pi}{2} < |\omega| \le \omega_m \end{cases} \end{aligned}\right\} \quad \text{for} \quad \gamma_6 < \gamma_3$$

where the minus signs take into account the reverse direction of traversal on certain portions of $\mathscr{S}_0^{(1)}$ and $\mathscr{S}_0^{(2)}$. These formulas can now be combined into the single formula

$$M^{\pm}(\omega) = \mu(T^{\pm}(\omega)) \operatorname{sgn}\left[\frac{\pi}{2} \pm |\omega| \operatorname{sgn}(\gamma_3 - \gamma_6)\right] \quad \text{for} \quad -\omega_m \le \omega \le \omega_m \tag{77}$$

where

$$\operatorname{sgn} x = +1 \qquad x > 0$$

$$\operatorname{sgn} x = -1 \qquad x < 0$$

In view of the mapping $T \to z$ defined by equation (50), this completes the solution of the problem since equation (65) determines ζ_1^{I} and ζ_1^{II} in terms of the known function Θ.

Expression of first-order potential in terms of Θ. - It is also convenient to have an expression for w_1^{I} in terms of Θ. In order to obtain this, note that it follows from the first and second equations (10) that

$$\zeta_1^{I} = \frac{dw_1^{I}}{dz} = \frac{dw_1^{I}}{dT}\frac{dT}{dw_0}\zeta_0$$

Hence,

$$\frac{dw_1^{I}}{dT} = \frac{dw_0}{dT}\frac{\zeta_1^{I}}{\zeta_0}$$

and equation (65) shows that

$$\frac{dw_1^{I}}{dT} = \Theta^{I}(T)\frac{dw_0}{dT} + \frac{1}{2}\frac{dw_0}{dT} \tag{78}$$

Note that $z = \ell e^{-i\pi\lambda}$ when $T = -\gamma_3$; and therefore equation (6) implies that both $w_1^I(T)$ and $w_0(T)$ vanish when $T = -\gamma_3$. Hence, integrating equation (78) between $T = -\gamma_3$ and T yields

$$w_1^I(T) = \int_{-\gamma_3}^{T} \Theta^I(T) \frac{dw_0}{dT} dT + \frac{1}{2} w_0(T) \tag{79}$$

Volume flow in jet. - Let Q denote the dimensionless volume flow per unit width through the jet. It follows from the definition of the stream function that, to within an error of $O(\epsilon^2)$,

$$Q = \mathcal{I}m\left[w_0(-\gamma_3 + i0) + \epsilon w_1^I(-\gamma_3 + i0)\right] - \mathcal{I}m\left[w_0(\gamma_6 + i0) + \epsilon w_1^I(\gamma_6 + i0)\right] + O(\epsilon^2)$$

On using equation (19) for $w_0(\gamma_6 + i0)$ and the fact that $w_1^I(T)$ and $w_0(T)$ both vanish at $T = -\gamma_3$, this becomes

$$Q = 1 - \epsilon\, \mathcal{I}m\, w_1^I(\gamma_6 + i0) + O(\epsilon^2)$$

Substituting equation (79) into this expression and using equation (19) again shows that

$$Q = 1 + \frac{\epsilon}{2} - \epsilon\, \mathcal{I}m \int_{-\gamma_3}^{\gamma_6} \Theta^I(T) \frac{dw_0}{dT} dT + O(\epsilon^2)$$

On substituting in equation (18), this becomes

$$Q = 1 + \frac{\epsilon}{2} + \frac{\epsilon}{\pi\gamma_3\gamma_6}\, \mathcal{I}m \int_{-\gamma_3}^{\gamma_6} \Theta^I(T) \frac{(T + \gamma_3)(T - \gamma_6)}{T} dT + O(\epsilon^2) \tag{80}$$

In view of the singularity in the denominator, this integral must first be carried out over the path of integration shown in figure 10 and then the limit $\epsilon_0 \to 0$ can be taken. Per-

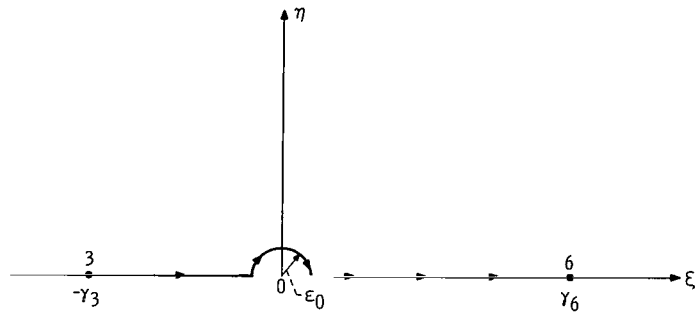

Figure 10. - Path of integration for equation (80) in T-plane.

forming these operations yields

$$\frac{1}{\pi\gamma_3\gamma_6}\int_{-\gamma_3}^{\gamma_6}\Theta^I(T)\,\frac{(T+\gamma_3)(T-\gamma_6)}{T}\,dT$$

$$=\frac{1}{\pi\gamma_3\gamma_6}\,\mathscr{P}.\mathscr{V}.\int_{-\gamma_3}^{\gamma_6}\Theta^I(\xi)\,\frac{(\xi+\gamma_3)(\xi-\gamma_6)}{\xi}\,d\xi+i\Theta^I(0)$$

Since $\Theta^I(\xi + i0)$ is real, equation (80) becomes

$$Q = 1 + \frac{\epsilon}{2} + \epsilon\Theta^I(0) + O(\epsilon^2) \tag{81}$$

Since the flow far downstream of the jet becomes uniform and since $\lim_{Z\to\infty}\zeta^{II}(z) = 1$, it follows from equation (2) and figure 2 that $\lim_{X\to\infty}\zeta^I(z) = \sqrt{1+\epsilon}$. Therefore, continuity requirements dictate that the dimensionless net volume flow through the jet Q be equal to $\delta\sqrt{1+\epsilon}$. Upon expanding this in powers of ϵ we find with the aid of the expansions in equation (12) that

$$Q = (1 + \epsilon\delta_1 + \ldots)\left(1 + \frac{1}{2}\epsilon + \ldots\right)$$

or

$$Q = 1 + \epsilon\left(\frac{1}{2} + \delta_1\right) \tag{82}$$

Hence, equating like powers of ϵ in equations (81) and (82) shows that

$$\delta_1 = \Theta^I(0) \tag{83}$$

Since equation (50) sets up a one-to-one correspondence between points in the physical plane and points in the T-plane, it is clear that equations (65), (75), and (79) can be used to compute the first-order perturbation to the velocity and stream function at each point of the physical plane within the jet.

Because of the fact that once the shape of the jet is known it is quite easy to sketch in the streamline patterns, the most important quantities to be obtained from the analysis are the shapes of the curves $S^{(1)}$ and $S^{(2)}$ (see fig. 2) in the physical plane.

Coordinates of slip lines. - In view of the one-to-one nature of mapping involved, if $\mathcal{I}m\, w^I(z) = 0$, then z must be a point on the streamline that passes through the point 3 in figure 2. In addition, since the velocity potential is increasing in the direction $3 \rightarrow 1$ along the slip line $S^{(1)}$, it is clear that, if $\mathcal{R}e\, w^I(z) > \mathcal{R}e\, w^I(\ell e^{-i\pi\lambda}) = 0$, then z must be a point on $S^{(1)}$. Now it is easy to see from the zeroth-order solution that $\mathcal{I}m\, w_0\left[z_0^{(1)}\right] = 0$ and $\mathcal{R}e\, w_0\left[z_0^{(1)}\right] \geq 0$ for any point $z_0^{(1)} \in S_0^{(1)}$. These considerations imply that the point $z^{(1)} = z_0^{(1)} + \epsilon z_1^{(1)}$ will be on the first-order position of $S^{(1)}$ if we let $z^{(1)}$ satisfy the equation

$$w^I\left[z^{(1)}\right] = w_0\left[z_0^{(1)}\right]\left(1 + \frac{\epsilon}{2}\right) \tag{84}$$

This equation shows that when $z_0^{(1)} = \ell e^{-i\pi\lambda}$, $w^I\left[z^{(1)}\right] = 0$ and that $\mathcal{R}e\, w^I\left[z^{(1)}\right] \rightarrow \infty$ as $z_0^{(1)} \rightarrow \infty$. Hence, the point $z^{(1)}$ traverses the slip line $S^{(1)}$ (to first order in ϵ) as $z_0^{(1)}$ traverses the zeroth-order slip line $S_0^{(1)}$.

Analogous considerations show that the point $z^{(2)} = z_0^{(2)} + \epsilon z_1^{(2)}$, which is determined by the equation

$$w^I\left[z^{(2)}\right] - w^I(-r - ih) = \left\{w_0\left[z_0^{(2)}\right] - w_0(-r - ih)\right\}\left(1 + \frac{\epsilon}{2}\right) \tag{85}$$

traverses the slip line $S^{(2)}$ to within first-order terms as the point $z_0^{(2)}$ traverses the zeroth-order slip line $S_0^{(2)}$. By substituting equations (84) and (85) into the expansion given in equation (52), the first-order distances $z_1^{(1)}$ and $z_1^{(2)}$ from the zeroth-order slip lines to the actual slip lines are found to be, respectively,

$$z_1^{(1)} = -\frac{1}{\zeta_0(T)}\left[w_1^I(T) - \frac{1}{2}w_0(T)\right] \quad \text{for } T \in \mathcal{S}_0^{(1)} \tag{86}$$

$$z_1^{(2)} = -\frac{1}{\zeta_0(T)}\left[w_1^I(T) - w_1^I(\gamma_6 + i0) - \frac{1}{2}w_0(T) + \frac{1}{2}w_0(\gamma_6 + i0)\right] \quad \text{for } T \in \mathscr{S}_0^{(2)} \tag{87}$$

where the fact has been used that the curves $S_0^{(1)}$ and $S_0^{(2)}$ in the physical plane are the conformal images under the mapping $T \to z$ defined by equation (50) of the curves $\mathscr{S}^{(1)}$ and $\mathscr{S}^{(2)}$, respectively, in the T-plane. This also shows that

$$z^{(1)} = z(T) + \epsilon z_1^{(1)}(T) + O(\epsilon^2) \quad \text{for } T \in \mathscr{S}_0^{(1)} \tag{88}$$

$$z^{(2)} = z(T) + \epsilon z_1^{(2)}(T) + O(\epsilon^2) \quad \text{for } T \in \mathscr{S}_0^{(2)} \tag{89}$$

Substituting equations (86) and (87) into equations (88) and (89), respectively, and substituting equation (79) into the resulting expressions yield

$$z^{(1)} = z(T) - \frac{\epsilon}{\zeta_0(T)} \int_{-\gamma_3}^{T} \Theta^I(T) \frac{dw_0}{dT}\, dT \quad \text{for } T \in \mathscr{S}_0^{(1)} \tag{90}$$

$$z^{(2)} = z(T) - \frac{\epsilon}{\zeta_0(T)} \int_{\gamma_6}^{T} \Theta^I(T) \frac{dw_0}{dT}\, dT \quad \text{for } T \in \mathscr{S}_0^{(2)} \tag{91}$$

where the contour of integration can be taken along $\mathscr{S}_0^{(1)}$ and $\mathscr{S}_0^{(2)}$ provided that $\Theta^I(T)$ is interpreted as the limiting value of $\Theta(T)$ as T approaches $\mathscr{S}_0^{(1)}$ and $\mathscr{S}_0^{(2)}$ from within D^I.

Static pressure distributions in jet and outer flow. - It follows from the first two expansions in equation (9) that

$$\left|\zeta^\nu(z)\right|^2 = \left|\zeta_0(z) + \epsilon\zeta_1^\nu(z) + O(\epsilon^2)\right|^2 = \left|\zeta_0(z)\right|^2 + 2\epsilon\left|\zeta_0(z)\right|^2 \mathcal{R}e\frac{\zeta_1^\nu(z)}{\zeta_0(z)} + O(\epsilon^2) \quad \text{for } \nu = I, II$$

Substituting equation (65) in this equation shows that the magnitude of the velocity is given to terms of order ϵ^2 by

$$\left|\zeta^I(T)\right|^2 = \left|\zeta_0(T)\right|^2\left[1 + \epsilon + 2\epsilon\Theta^I(T)\right] + O(\epsilon^2) \quad \text{for } T \in \mathscr{D}^I \tag{92}$$

$$\left|\zeta^{II}(T)\right|^2 = \left|\zeta_0(T)\right|^2\left[1 + 2\epsilon\Theta^{II}(T)\right] + O(\epsilon^2) \quad \text{for } T \in \mathscr{D}^{II} \tag{93}$$

It follows from Bernoulli's equation and equation (1) that within the jet

$$\frac{p - p_\infty}{\frac{1}{2}\rho V_\infty^2} = 1 + \epsilon - \left|\zeta^{I}\right|^2$$

and within the main stream

$$\frac{p - p_\infty}{\frac{1}{2}\rho V_\infty^2} = 1 - \left|\zeta^{II}\right|^2$$

Hence, substituting equations (92) and (93) in these equations gives the following expressions for the static pressure distributions:

$$\frac{p - p_\infty}{\frac{1}{2}\rho V_\infty^2} = (1 + \epsilon)\left[1 - \left|\zeta_0(T)\right|^2\right] - 2\epsilon\left|\zeta_0(T)\right|^2 \Theta^{I}(T) \qquad \text{for } T \in \mathscr{D}^{I} \tag{94}$$

$$\frac{p - p_\infty}{\frac{1}{2}\rho V_\infty^2} = 1 - \left|\zeta_0(T)\right|^2 - 2\epsilon\left|\zeta_0(T)\right|^2 \Theta^{II}(T) \qquad \text{for } T \in \mathscr{D}^{II} \tag{95}$$

All necessary results have now been obtained. However, it is useful to rewrite some of these in more explicit form.

Explicit Formulas for Calculating Quantities of Physical Interest Along Boundaries

We shall now find the limiting values of $\Theta(T)$ in equation (76) as T approaches the contours $\mathscr{S}_0^{(1)}$ and $\mathscr{S}_0^{(2)}$. In order to do this we apply the Plemelj formulas (ref. 4), being sure to take into account the reversals in the directions of integration indicated in figure 8. Once this is done and the parametric equations (47) and (48) of $\mathscr{S}_0^{(1)}$ and $\mathscr{S}_0^{(2)}$ are inserted into the results, we obtain

$$\left.\begin{aligned}\Theta(T) = \begin{cases}\Theta^-(\omega) & \text{with } -\omega_m \le \omega < 0 \text{ for } |T| \le \rho_m \\ \Theta^+(\omega) & \text{with } -\omega_m \le \omega < -\frac{\pi}{2} \text{ for } |T| \ge \rho_m\end{cases} \quad \text{for } T \in \mathscr{S}_0^{(1)} \\ \Theta(T) = \Theta^+(\omega) \quad \text{with } 0 < \omega < \frac{\pi}{2} \text{ for } T \in \mathscr{S}_0^{(2)}\end{aligned}\right\} \text{ for } \gamma_6 > \gamma_3 \tag{96}$$

$$\left.\begin{aligned}\Theta(T) = \Theta^-(\omega) \quad \text{with } -\frac{\pi}{2} < \omega < 0 \text{ for } T \in \mathscr{S}_0^{(1)} \\ \Theta(T) = \begin{cases}\Theta^+(\omega) & \text{with } 0 < \omega \le \omega_m \text{ for } |T| \le \rho_m \\ \Theta^-(\omega) & \text{with } \frac{\pi}{2} < \omega \le \omega_m \text{ for } |T| \ge \rho_m\end{cases} \quad \text{for } T \in \mathscr{S}_0^{(2)}\end{aligned}\right\} \text{ for } \gamma_6 < \gamma_3 \tag{97}$$

where we have put

$$\Theta^{\pm}(\omega) = \frac{1}{2}\mu\left[T^{\pm}(\omega)\right] + \frac{1}{2\pi i}\int_{-\omega_m}^{\omega_m} \frac{M^{\mp}(\tilde{\omega})}{T^{\mp}(\tilde{\omega}) - T^{\pm}(\omega)} \frac{dT^{\mp}(\tilde{\omega})}{d\tilde{\omega}}\, d\tilde{\omega}$$

$$+ \frac{\mathscr{P}.\mathscr{V}.}{2\pi i}\int_{-\omega_m}^{\omega_m} \frac{M^{\pm}(\tilde{\omega})}{T^{\pm}(\tilde{\omega}) - T^{\pm}(\omega)} \frac{dT^{\pm}(\tilde{\omega})}{d\tilde{\omega}}\, d\tilde{\omega} \tag{98}$$

The difference in sign between the $\mu(T^{\pm})$ term and the $M^{\pm}$ is due to the reversal in the direction in which the contour is traversed with increasing ω in certain regions. The fact that the proper sign is used in the $(1/2)\mu$ term can be verified by taking the limiting values directly in equation (75).

Upon differentiating equation (43) we find that

$$\frac{dT^{\pm}(\omega)}{d\omega} = \frac{i}{2}\frac{\gamma_6 - \gamma_3}{\cos^2\omega} \pm \frac{i\left(\gamma_6 - \gamma_3\right)^2 \sin^2\omega + 2\gamma_6\gamma_3 \cos\omega(\sin\omega\cos\omega e^{i\omega} - \omega e^{-i\omega})}{2\cos^2\omega \sin^2\omega \sqrt{\left(\gamma_6 - \gamma_3\right)^2 + 4\gamma_6\gamma_3\omega\cot\omega}} \tag{99}$$

Coordinates of slip lines. - Now substituting equations (18), (50), and (96) into equations (90) and (91) and using equations (47) and (48) and figure 2(b), we find the following

parametric equations for the slip lines $\mathscr{S}_0^{(1)}$ and $\mathscr{S}_0^{(2)}$ correct to first order in ϵ

$$z^{(1)} = \begin{cases} \ell e^{-i\pi\lambda} + z_0^-(\omega,0) + \dfrac{\epsilon}{\zeta_0^-(\omega)}\, z^-(\omega,0) & \text{for } -\omega_m \le \omega < 0 \\ \ell e^{-i\pi\lambda} + z_0^-(-\omega_m,0) + z_0^+(\omega,-\omega_m) + \dfrac{\epsilon}{\zeta_0^+(\omega)}\left[z^-(-\omega_m,0) + z^+(\omega,-\omega_m)\right] & \text{for } -\omega_m \le \omega < \dfrac{\pi}{2} \end{cases} \Bigg\} \text{for } \gamma_6 > \gamma_3 \qquad (100)$$

$$z^{(2)} = -(r + ih) + z_0^+(\omega,0) + \frac{\epsilon}{\zeta_0^+(\omega)}\, z^+(\omega,0) \quad \text{for } 0 < \omega < \frac{\pi}{2}$$

(100)

$$z^{(1)} = \ell e^{-i\pi\lambda} + z_0^-(\omega,0) + \frac{\epsilon}{\zeta_0^-(\omega)}\, z^-(\omega,0) \quad \text{for } -\frac{\pi}{2} < \omega < 0$$

$$z^{(2)} = \begin{cases} -(r + ih) + z_0^+(\omega,0) + \dfrac{\epsilon}{\zeta_0^+(\omega)}\, z^+(\omega,0) & \text{for } 0 < \omega \le \omega_m \\ -(r + ih) + z_0^+(\omega_m,0) + z_0^-(\omega,\omega_m) + \dfrac{\epsilon}{\zeta_0^-(\omega)}\left[z^+(\omega_m,0) + z^-(\omega,\omega_m)\right] & \text{for } \dfrac{\pi}{2} < \omega \le \omega_m \end{cases} \Bigg\} \text{for } \gamma_6 < \gamma_3 \qquad (101)$$

where we have put

$$z_0^{\pm}(\omega_1,\omega_0) = -\frac{1}{\pi\gamma_3\gamma_6}\int_{\omega_0}^{\omega_1} \frac{1}{\zeta_0^{\pm}(\omega)}\,\frac{\left[T^{\pm}(\omega) + \gamma_3\right]\left[T^{\pm}(\omega) - \gamma_6\right]}{T^{\pm}(\omega)}\,\frac{dT^{\pm}(\omega)}{d\omega}\,d\omega \qquad (102a)$$

$$z^{\pm}(\omega_1,\omega_0) = \frac{1}{\pi\gamma_3\gamma_6}\int_{\omega_0}^{\omega_1} \Theta^{\pm}(\omega)\,\frac{\left[T^{\pm}(\omega) + \gamma_3\right]\left[T^{\pm}(\omega) - \gamma_6\right]}{T^{\pm}(\omega)}\,\frac{dT^{\pm}(\omega)}{d\omega}\,d\omega \qquad (102b)$$

and

$$\zeta_0^{\pm}(\omega) = \left[\frac{T^{\pm}(\omega) + \gamma_4}{T^{\pm}(\omega) + 1}\right]^{\lambda} \qquad (103)$$

Summary of Equations

For convenience, the most important equations are now summarized.

Relation between β-values and dimensionless length of deflecting plate:

$$\ell = \frac{\left(1 - \beta_5\right)^3}{\pi(\beta_3 + \beta_5)(\beta_6 - \beta_5)} \int_0^{\beta_3} \frac{1}{\sigma^\lambda} \frac{(\beta_3 - \sigma)(\beta_6 + \sigma)}{(1 + \sigma)^3(\beta_5 + \sigma)} d\sigma \tag{31}$$

Relation between β-values and dimensionless orifice offset distance:

$$r = \frac{\left(1 - \beta_5\right)^3}{\pi(\beta_3 + \beta_5)(\beta_6 - \beta_5)} \mathscr{P}.\mathscr{V}. \int_0^{\beta_6} \frac{1}{\sigma^\lambda} \frac{(\beta_3 + \sigma)(\sigma - \beta_6)}{(\sigma - \beta_5)(1 - \sigma)^3} d\sigma \tag{33}$$

$$(\beta_5 - \beta_6)(\beta_5 + \beta_3)\left[1 - \frac{1}{\beta_5^\lambda} - \lambda(\beta_5 - 1)\right] = \frac{\lambda(\lambda + 1)}{2}\left(\beta_5 - 1\right)^2(\beta_3 + 1)(\beta_6 - 1) - \lambda\left(\beta_5 - 1\right)^3 \tag{32}$$

Dimensionless orifice width (reciprocal of dimensionless asymptotic zeroth-order jet width):

$$h = \frac{1}{\beta_5^\lambda} \tag{34}$$

$$\left.\begin{aligned} \gamma_3 &= \frac{\beta_3 + \beta_5}{1 + \beta_3} \\ \gamma_4 &= \beta_5 \\ \gamma_6 &= \frac{\beta_6 - \beta_5}{1 - \beta_6} \end{aligned}\right\} \tag{28}$$

$$\left(\gamma_6 - \gamma_3\right)^2 \tan \omega_m + 4\gamma_3\gamma_6\omega_m = 0 \qquad \text{for} \quad \omega_m \geq 0 \tag{44}$$

$$T^{\pm}(\omega) = \frac{1}{2}\left[\gamma_6 - \gamma_3 \pm \sqrt{\left(\gamma_6 - \gamma_3\right)^2 + 4\gamma_3\gamma_6\omega \cot \omega}\right](1 + i \tan \omega) \qquad \text{for} \quad -\omega_m \leq \omega \leq \omega_m \tag{43}$$

$$\frac{dT^{\pm}(\omega)}{d\omega} = \frac{i}{2}\frac{\gamma_6 - \gamma_3}{\cos^2\omega} \pm \frac{i(\gamma_6 - \gamma_3)^2 \sin^2\omega + 2\gamma_6\gamma_3 \cos\omega(\sin\omega\cos\omega e^{i\omega} - \omega e^{-i\omega})}{2\cos^2\omega \sin^2\omega \sqrt{(\gamma_6 - \gamma_3)^2 + 4\gamma_6\gamma_3\omega\cot\omega}} \quad (99)$$

$$\mu(T^{\pm}) = \frac{1}{2}\left[\left(\frac{|T^{\pm}|^2 + 2\,Re\,T^{\pm} + 1}{|T^{\pm}|^2 + 2\gamma_4\,Re\,T^{\pm} + \gamma_4^2}\right)^{\lambda} - 1\right] \quad (74)$$

$$M^{\pm}(\omega) = \mu[T^{\pm}(\omega)]\ \mathrm{sgn}\left[\frac{\pi}{2} \pm |\omega|\ \mathrm{sgn}(\gamma_3 - \gamma_6)\right] \quad (77)$$

$$\Theta^{\pm}(\omega) = \frac{1}{2}\mu[T^{\pm}(\omega)] + \frac{1}{2\pi i}\int_{-\omega_m}^{\omega_m} \frac{M^{\mp}(\tilde{\omega})}{T^{\mp}(\tilde{\omega}) - T^{\pm}(\omega)}\frac{dT^{\mp}(\tilde{\omega})}{d\tilde{\omega}}\,d\tilde{\omega}$$

$$+ \frac{\mathcal{P}.\mathcal{V}.}{2\pi i}\int_{-\omega_m}^{\omega_m} \frac{M^{\pm}(\tilde{\omega})}{T^{\pm}(\tilde{\omega}) - T^{\pm}(\omega)}\frac{dT^{\pm}(\tilde{\omega})}{d\tilde{\omega}}\,d\tilde{\omega} \quad (98)$$

$$\Theta(\xi + i0) = Re\,\frac{1}{\pi i}\left[\int_0^{\omega_m} \frac{M^{+}(\omega)}{T^{+}(\omega) - \xi}\frac{dT^{+}(\omega)}{d\omega}\,d\omega + \int_0^{\omega_m} \frac{M^{-}(\omega)}{T^{-}(\omega) - \xi}\frac{dT^{-}(\omega)}{d\omega}\,d\omega\right] \quad (108)$$

$$z_0^{\pm}(\omega_1, \omega_0) = -\frac{1}{\pi\gamma_3\gamma_6}\int_{\omega_0}^{\omega_1} \frac{1}{\zeta_0^{\pm}(\omega)}\frac{[T^{\pm}(\omega) + \gamma_3][T^{\pm}(\omega) - \gamma_6]}{T^{\pm}(\omega)}\frac{dT^{\pm}(\omega)}{d\omega}\,d\omega \quad (102a)$$

$$z^{\pm}(\omega_1, \omega_0) = \frac{1}{\pi\gamma_6\gamma_3}\int_{\omega_0}^{\omega_1} \Theta^{\pm}(\omega)\frac{[T^{\pm}(\omega) + \gamma_3][T^{\pm}(\omega) - \gamma_6]}{T^{\pm}(\omega)}\frac{dT^{\pm}(\omega)}{d\omega}\,d\omega \quad (102b)$$

$$\zeta_0^{\pm}(\omega) = \left[\frac{T^{\pm}(\omega) + \gamma_4}{T^{\pm}(\omega) + 1}\right]^{\lambda} \quad (103)$$

Coordinates of the slip lines:

$$z^{(1)} = \ell e^{-i\pi\lambda} + z_0^-(\omega,0) + \frac{\epsilon}{\zeta_0^-(\omega)} z^-(\omega,0) \quad \text{for } -\frac{\pi}{2} < \omega < 0$$

$$z^{(2)} = \begin{cases} -(r + ih) + z_0^+(\omega,0) + \dfrac{\epsilon}{\zeta_0^+(\omega)} z^+(\omega,0) & \text{for } 0 < \omega \le \omega_m \\ -(r + ih) + z_0^+(\omega_m,0) + z_0^-(\omega,\omega_m) + \dfrac{\epsilon}{\zeta_0^-(\omega)} \left[z^+(\omega_m,0) + z^-(\omega,\omega_m) \right] & \text{for } \frac{\pi}{2} < \omega \le \omega_m \end{cases} \quad \text{for } \gamma_6 < \gamma_3 \tag{100}$$

$$z^{(1)} = \begin{cases} \ell e^{-i\pi\lambda} + z_0^-(\omega,0) + \dfrac{\epsilon}{\zeta_0^-(\omega)} z^-(\omega,0) & \text{for } -\omega_m \le \omega < 0 \\ \ell e^{-i\pi\lambda} + z_0^-(-\omega_m,0) + z_0^+(\omega,-\omega_m) + \dfrac{\epsilon}{\zeta_0^+(\omega)} \left[z^-(-\omega_m,0) + z^+(\omega,-\omega_m) \right] & \text{for } -\omega_m < \omega < \frac{\pi}{2} \end{cases} \quad \text{for } \gamma_6 > \gamma_3 \tag{101}$$

$$z^{(2)} = -(r + ih) + z_0^+(\omega,0) + \frac{\epsilon}{\zeta_0^+(\omega)} z^+(\omega,0) \quad \text{for } 0 < \omega < \frac{\pi}{2}$$

OUTLINE OF CALCULATIONAL PROCEDURE

The numerical evaluation of the analytical results was carried out by using complex arithmetic. Hence, there was no need to analytically separate the real and imaginary parts of the various equations which were used. In order to evaluate the final expressions, certain parameters and results which are completely determined by the zeroth-order solution must be found. The procedures involved in accomplishing this will therefore be discussed first.

As shown by equations (28) and (31) to (34) (refer to the section Summary of Equations), the physical quantities ℓ, r, and h are related implicitly to the parameters β_3, β_5, and β_6 in a complicated manner; and the parameters γ_3, γ_4, and γ_6 are in turn related to the β's. For a given deflection angle $\lambda = \alpha/\pi$, it is convenient to choose values for the jet contraction ratio $\Delta_0/H = 1/h$ and for β_3. Then from equation (34) the parameter β_5 is found, and the parameters γ_3 and γ_4 are obtained from the first two equations (28). Equation (32) can then be solved for β_6; and with all the β's known, ℓ, r, and γ_6 are obtained from equations (31), (33), and the last of equations (28). Since 1/h and β_3 are convenient computer input parameters, grids can be prepared as shown in figure 11 to aid in choosing input parameters from the physical data. Note that the magnitude of the orifice width H is arbitrary. The values in figure 11 are for positive

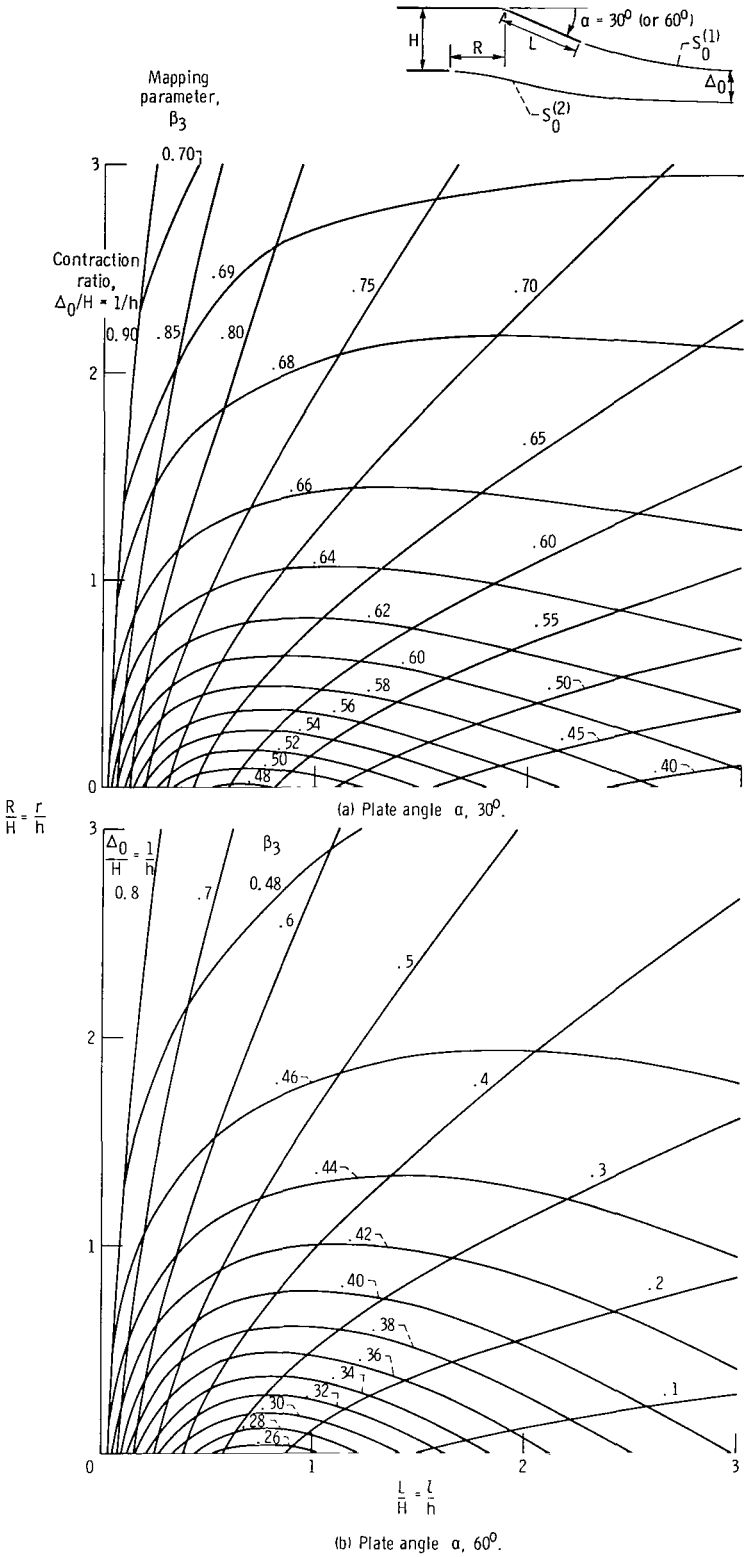

(a) Plate angle α, 30°.

(b) Plate angle α, 60°.

Figure 11. - Relation between geometric parameters with positive values of angle α to contraction ratio 1/h and mapping parameter β_3.

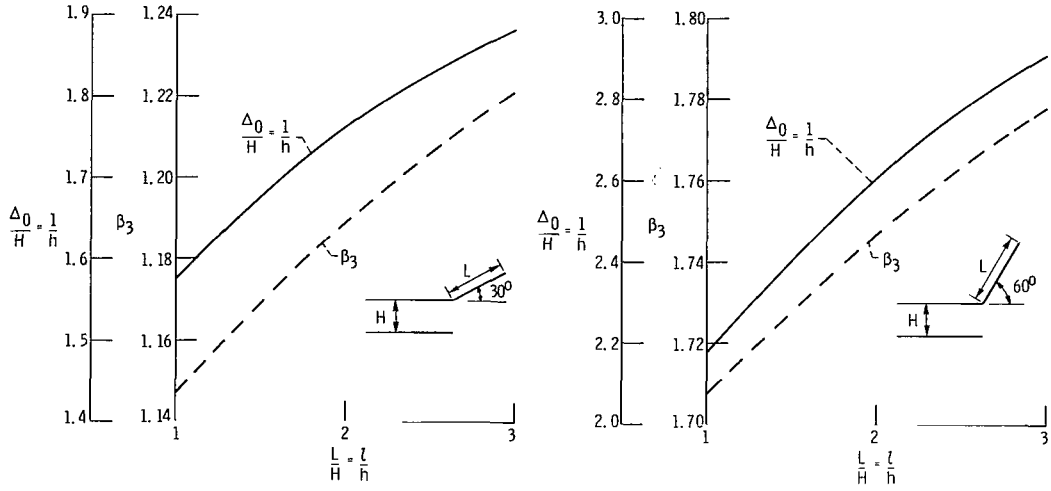

(a) Plate angle α, -30^0.

(b) Plate angle α, -60^0.

Figure 12. - Relation of jet contraction ratio and mapping parameter β_3 to geometric quantities for negative values of angle α.

values of the angle α. Some results will also be given for negative α and zero orifice offset distance (R = 0), with the relations between Δ_0/H, β_3, and L/H for these cases given in figure 12.

Now that the physical parameters have been expressed in terms of the γ's, the coordinates of the jet bounding slip lines can be obtained. The transcendental equation (44) is first solved for ω_m. With the γ's known, the functions $T^{\pm}(\omega)$ and $dT^{\pm}/d\omega$ can be evaluated from equations (43) and (99) and then $\mu(T^{\pm})$ and $M^{\pm}(\omega)$ can be obtained from equations (74) and (77). These quantities are used in equations (98) and (103) to obtain $\Theta^{\pm}(\omega)$ and $\zeta_0^{\pm}(\omega)$. Then the integrations in equations (102a) and (102b) are carried out to yield the functions $z_0^{\pm}(\omega_1, \omega_0)$ and $z^{\pm}(\omega_1, \omega_0)$. For various values of the total pressure difference parameter ϵ, the coordinates along the slip lines can be found from equations (100) and (101) depending on whether γ_3 is larger or smaller than γ_6.

DISCUSSION

The objective of this report was to develop a technique to analyze the flow interaction when a two-dimensional jet is injected between two moving streams. Such an analysis must account for conditions where the total pressure in the jet differs from that in the outer stream. The analysis must also account for the variation of static pressure along the jet bounding slip lines, a feature not taken into account in classical free-jet analyses. The analysis was applied to the configurations shown in figure 1, and the figures that are presented in the following discussion will show typical slip line patterns. In all the figures the geometry has been nondimensionalized by the orifice width H shown in figure 2(a)

Positive Deflection Angles

First, consider the results for positive values of the angle α. Two values, $\alpha = 30^{o}$ and 60^{o}, were considered; and for each of these, results are presented for three dimensionless plate lengths L/H = 1, 2, and 3 and two orifice offset distances R/H = 1 and 2. The results are shown in figures 13 and 14, which correspond to $\alpha = 30^{o}$ and 60^{o}, respectively. Table I gives the specific values of the parameters Δ_0/H and β_3 for these cases.

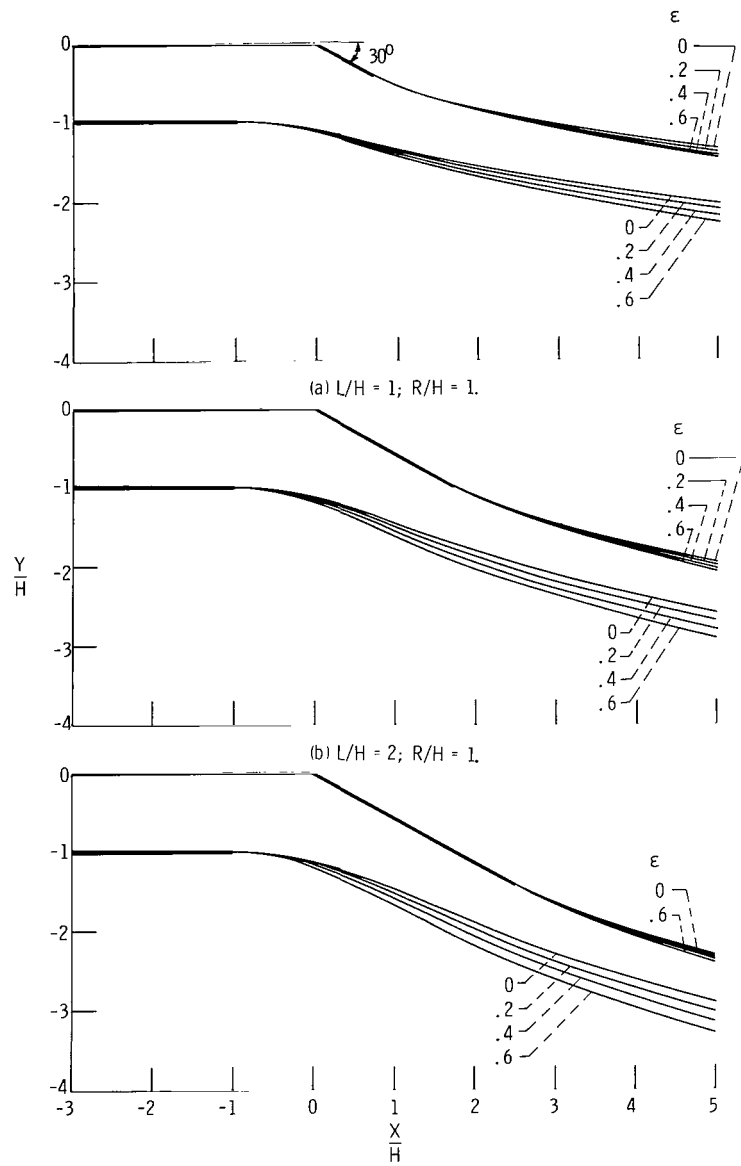

(a) L/H = 1; R/H = 1.

(b) L/H = 2; R/H = 1.

(c) L/H = 3; R/H = 1.

Figure 13. - Jet slip line boundaries for outlet with 30° plate deflection angle.

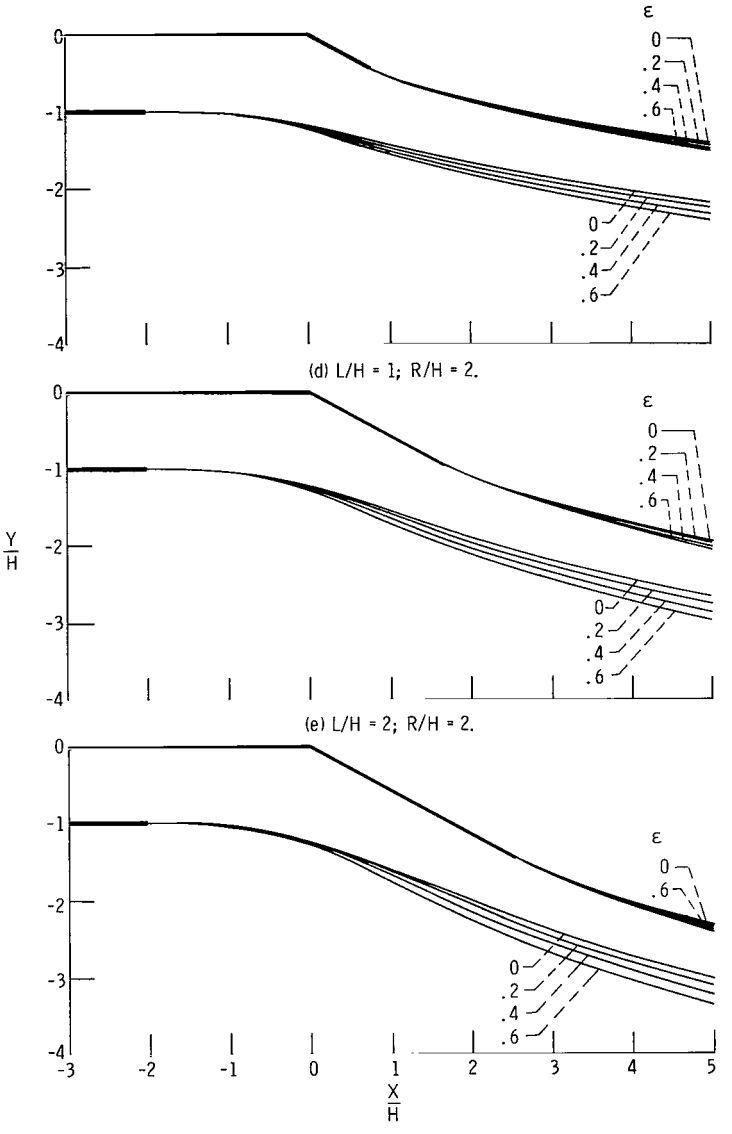

(d) L/H = 1; R/H = 2.

(e) L/H = 2; R/H = 2.

(f) L/H = 3; R/H = 2.

Figure 13. - Concluded.

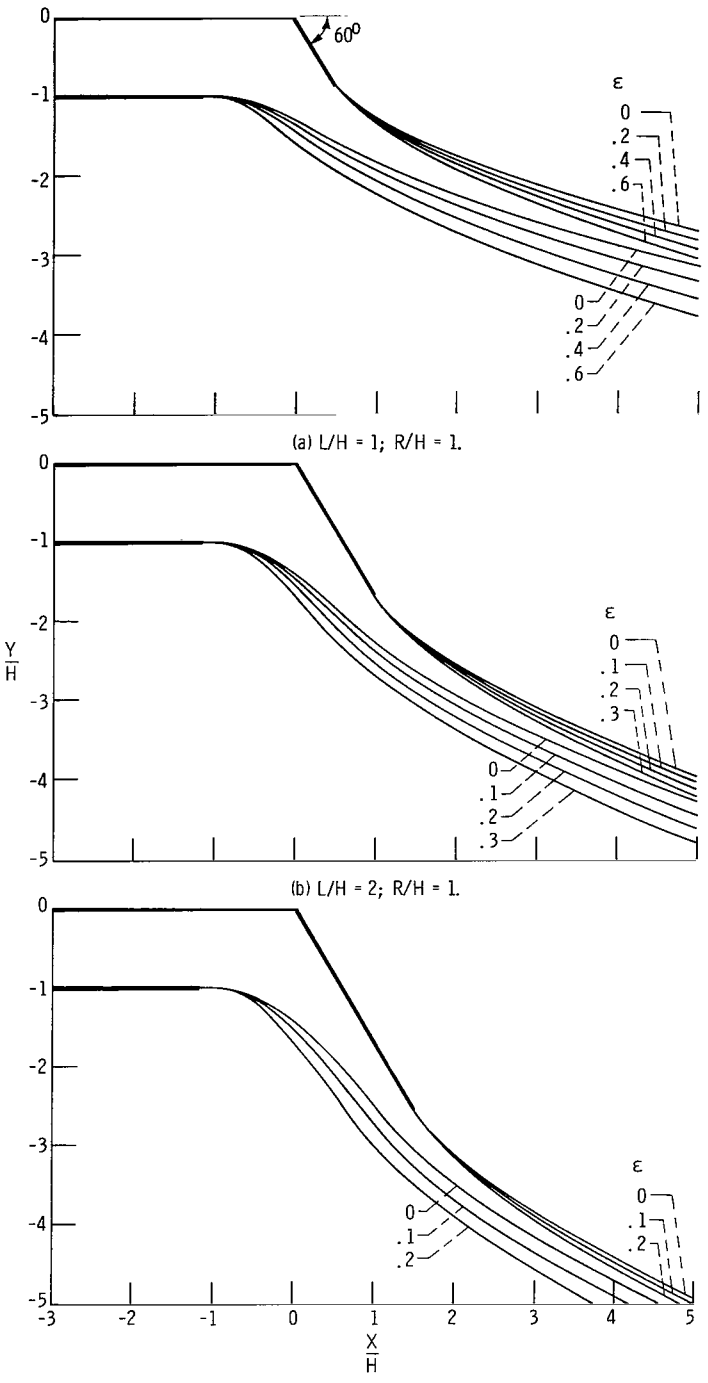

(a) L/H = 1; R/H = 1.

(b) L/H = 2; R/H = 1.

(c) L/H = 3; R/H = 1.

Figure 14. - Jet slip line boundaries for outlet with 60^0 plate deflection angle.

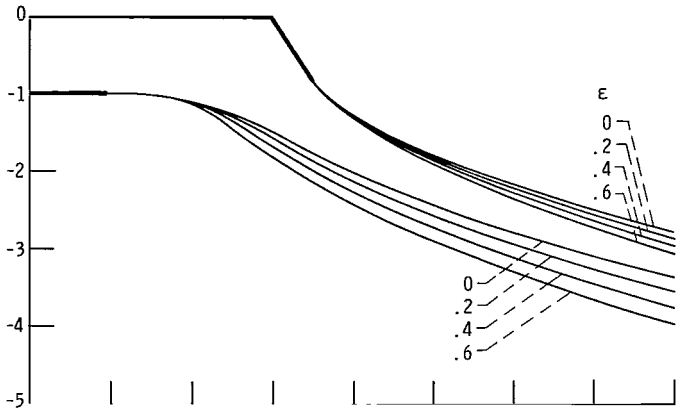

(d) L/H = 1; R/H = 2.

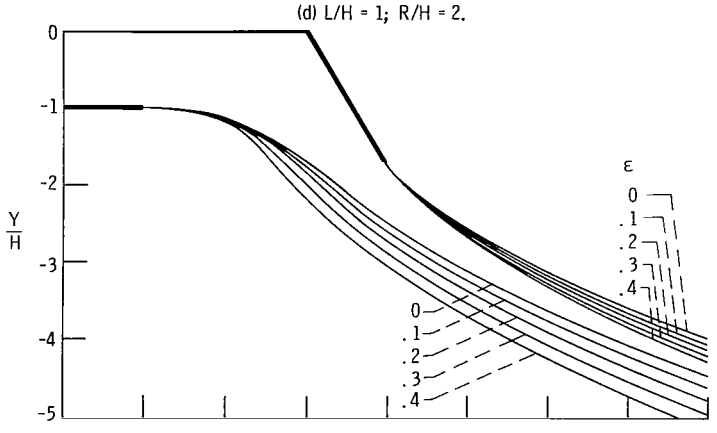

(e) L/H = 2; R/H = 2.

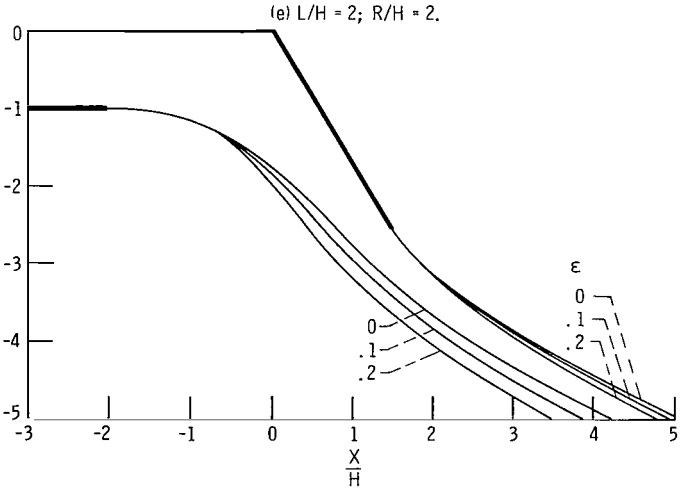

(f) L/H = 3; R/H = 2.

Figure 14. - Concluded.

TABLE I. - ZEROTH-ORDER CONTRACTION RATIO AND β_3 AS FUNCTION OF GEOMETRIC PARAMETERS

Plate angle, α	Dimensionless plate length, L/H	Dimensionless offset distance, R/H	Zeroth-order contraction ratio, Δ_0/H	Mapping parameter, β_3	Figure
30	1	1	0.67673	0.63568	13(a)
↓	2	1	.59198	.64244	13(b)
	3	1	.54410	.65225	13(c)
	1	2	.75562	.67882	13(d)
	2	2	.68060	.67645	13(e)
	3	2	.63411	.67821	13(f)
60	1	1	.40540	.42008	14(a)
↓	2	1	.27970	.42814	14(b)
	3	1	.22175	.44116	14(c)
	1	2	.53905	.46570	14(d)
	2	2	.41110	.46160	14(e)
	3	2	.34041	.46369	14(f)
-30	1	0	1.57478	1.14683	15(a)
-30	2	0	1.76227	1.18917	15(b)
-30	3	0	1.88322	1.22134	15(c)
-60	1	0	2.17472	1.70739	16(a)
-60	2	0	2.60760	1.74679	16(b)
-60	3	0	2.90804	1.77788	16(c)

The ratio Δ_0/H is the zeroth-order contraction ratio of the jet. The results in either table I or figure 11 show how this contraction ratio decreases as either L/H is increased (with R/H fixed) or R/H is decreased (with L/H fixed). Increasing the angle α also causes Δ_0/H to decrease, as would be expected from the geometrical configuration.

Figures 13 and 14 show the slip lines for various values of the total pressure difference parameter ϵ. It follows from the nature of the asymptotic expansions in equation (9) that the parameter ϵ cannot be so large as to cause a large deviation in the slip lines from their zeroth-order positions. As ϵ is increased, the total pressure in the jet is increased above that in the stream, as shown by equation (1). This produces two effects on the slip line configuration: the jet width expands as ϵ increases; and the jet deflection tends to persist over a longer path, that is, it is more difficult for the outer stream to turn the jet into the horizontal direction, resulting in an increase in jet penetration.

Negative Deflection Angles

Results for the type of geometry shown in figure 1(b) can be obtained by letting the angle α be negative. The slip lines are shown in figures 15 and 16. The validity of the

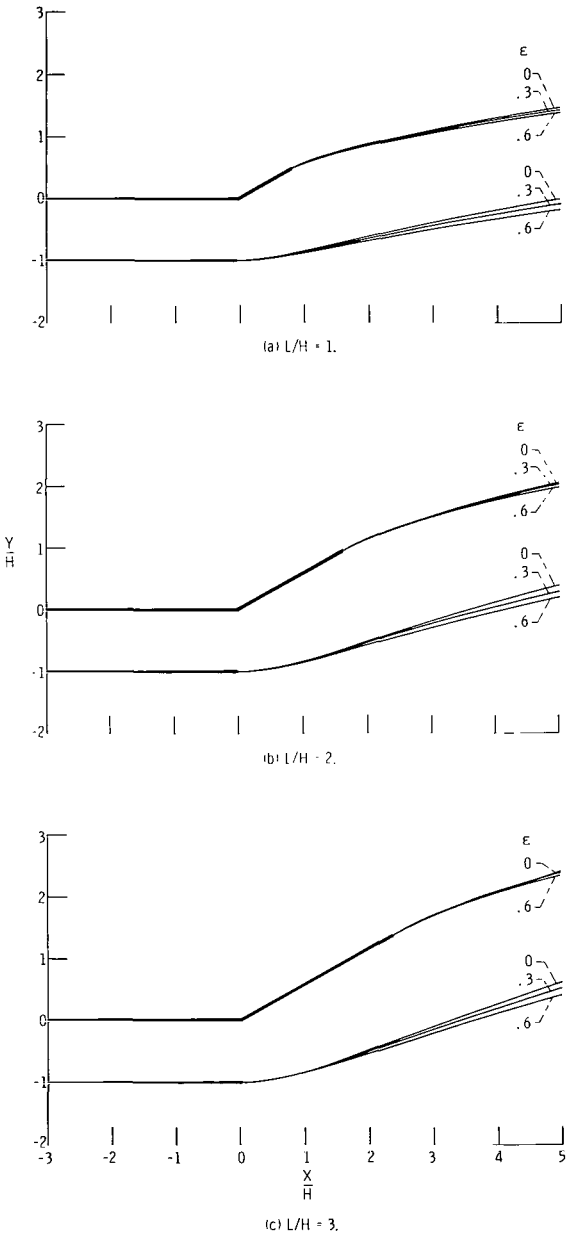

Figure 15. - Jet slip line boundaries for zero orifice offset distance and a plate deflection angle of -30^{0}.

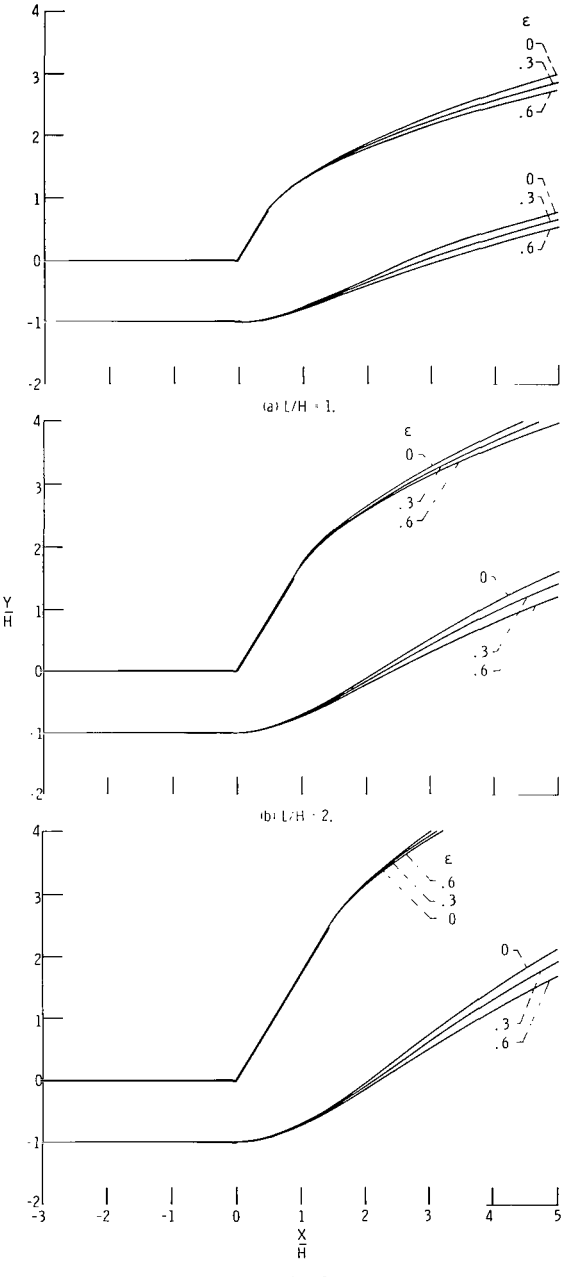

Figure 16. - Jet slip line boundaries for zero orifice offset distance and a plate deflection angle of -60^{0}.

results depend on the flow remaining attached to the upper boundary by means of the Coanda effect, and this attachment can be promoted by boundary layer control.

All the results in figures 15 and 16 are for zero offset of the orifice lip (R/H = 0). The contraction ratio Δ_0/H (see table I) is larger than unity in this instance as the flap is expanding the jet by virtue of the attachment of the upper jet streamline. When the value of ϵ is increased, the width of the jet tends to expand and its path is more horizontal.

CONCLUDING REMARKS

An analytical technique was devised for determining the flow characteristics of an inviscid two-dimensional jet interacting along both of its boundaries with an outer mainstream flow. The velocity variations in the outer flow produce a priori unknown static pressure variations along the jet boundaries, a condition not accounted for in classical jet analyses, which ordinarily have a uniform static pressure (stationary outer flow) along the jet free streamlines. The analysis also accounted for the total pressure in the jet differing from the free-stream total pressure, with the restriction that this difference does not become too large in comparison with the free-stream kinetic energy head.

Specific results were carried out for two configurations of the channel used to inject the jet into the stream, and the shapes of the bounding jet slip lines were calculated. The results show how the jet penetration and contraction or expansion depend on the total pressure in the jet relative to that in the free stream.

Lewis Research Center,
National Aeronautics and Space Administration,
Cleveland, Ohio, February 23, 1972,
136-13.

APPENDIX - SYMBOLS

b	characteristic length, put equal to Δ_0
C_0	integration contour, fig. 7
D^I, D^{II}	flow regions in physical plane
D_0^I, D_0^{II}	zeroth-order flow regions in physical plane
$\mathscr{D}^I, \mathscr{D}^{II}$	flow regions in T-plane
H	orifice width
h	dimensionless orifice width, H/Δ_0
L	length of plate at angle to flow
l	L/Δ_0
$M^{\pm}$	defined in eq. (77)
O	order symbol
P_∞	total pressure in main stream
P_j	total pressure in jet
$\mathscr{P}.\mathscr{V}.$	Cauchy principal value
p	static pressure
p_∞	static pressure far upstream from orifice
Q	volume flow through jet
R	orifice offset distance
r	R/Δ_0
$S^{(1)}, S^{(2)}$	upper and lower slip lines (in physical plane)
$S_0^{(1)}, S_0^{(2)}$	zeroth-order position of upper and lower slip lines
$\mathscr{S}^{(1)}, \mathscr{S}^{(2)}$	slip lines in T-plane
T	intermediate variable, $T = \xi + i\eta$
$T^{\pm}$	defined in eq. (43)
U	X-component of velocity
u	U/V_∞
V	Y-component of velocity
V_∞	free-stream velocity

v	V/V_∞
w	dimensionless complex potential, $W = \varphi + i\psi$
X	coordinate in physical plane
x	X/Δ_0
Y	coordinate in physical plane
y	Y/Δ_0
z	dimensionless complex physical coordinate, $z = x + iy$
$z^{\pm}$	defined by eq. (102)
$z^{(1)}, z^{(2)}$	dimensionless coordinates of points on slip lines
α	angle of plate relative to undisturbed main stream
$B(m, n)$	beta-function
$\beta_3, \beta_5, \beta_6$	parameters in Ω-plane
Γ	gamma-function
$\gamma_3, \gamma_4, \gamma_6$	parameters in T-plane
Δ	asymptotic jet width
δ	Δ/Δ_0
ϵ	$(P_j - P_\infty)/(1/2)\rho V_\infty^2$
ϵ_0	radius for contour integral in figs. 7 and 10
ζ	dimensionless complex conjugate velocity, $\zeta = u - iv$
η	coordinate in T-plane
Θ	defined in eq. (65)
$\Theta^{\pm}$	defined by eq. (98)
θ	polar coordinate in T-plane
θ_1, θ_2	solutions of trancendental eqs. (38)
λ	α/π
μ	defined by eq. (74)
ν	dummy index
ξ	coordinate in T-plane
ρ	density of fluid

σ coordinate in Ω-plane

τ coordinate in Ω-plane

Φ velocity potential

φ $\Phi/\Delta_0 V_\infty$

Ψ stream function

ψ $\Psi/\Delta_0 V_\infty$

Ω intermediate mapping variable, $\Omega = \sigma + i\tau$

ω parametric variable defined after eq. (40)

ω_m solution of trancendental eq. (44)

Subscripts:

0 zeroth-order quantity

1 first-order quantity

Superscripts:

I inside jet

II in main stream

1 on $S^{(1)}$

2 on $S^{(2)}$

$\bar{}$ complex conjugate

REFERENCES

1. Goldstein, Marvin E.; and Braun, Willis: Injection of an Inviscid Separated Jet at an Oblique Angle to a Moving Stream. NASA TN D-5460, 1969.
2. Birkhoff, Garrett; and Zarantonello, E. H.: Jets, Wakes, and Cavities. Academic Press, 1957.
3. Churchill, Ruel V.: Complex Variables and Applications. Second ed., McGraw-Hill Book Co., Inc., 1960.
4. Muskhelishvili, Nikolai I. (J. R. M. Radok, trans.): Singular Integral Equations. P. Noordhoff Ltd, 1953.

NASA-Langley, 1972 —— 1 E-6583

"The aeronautical and space activities of the United States shall be conducted so as to contribute . . . to the expansion of human knowledge of phenomena in the atmosphere and space. The Administration shall provide for the widest practicable and appropriate dissemination of information concerning its activities and the results thereof."

— NATIONAL AERONAUTICS AND SPACE ACT OF 1958

NASA SCIENTIFIC AND TECHNICAL PUBLICATIONS

TECHNICAL REPORTS: Scientific and technical information considered important, complete, and a lasting contribution to existing knowledge.

TECHNICAL NOTES: Information less broad in scope but nevertheless of importance as a contribution to existing knowledge.

TECHNICAL MEMORANDUMS: Information receiving limited distribution because of preliminary data, security classification, or other reasons.

CONTRACTOR REPORTS: Scientific and technical information generated under a NASA contract or grant and considered an important contribution to existing knowledge.

TECHNICAL TRANSLATIONS: Information published in a foreign language considered to merit NASA distribution in English.

SPECIAL PUBLICATIONS: Information derived from or of value to NASA activities. Publications include conference proceedings, monographs, data compilations, handbooks, sourcebooks, and special bibliographies.

TECHNOLOGY UTILIZATION PUBLICATIONS: Information on technology used by NASA that may be of particular interest in commercial and other non-aerospace applications. Publications include Tech Briefs, Technology Utilization Reports and Technology Surveys.

Details on the availability of these publications may be obtained from:

SCIENTIFIC AND TECHNICAL INFORMATION OFFICE

NATIONAL AERONAUTICS AND SPACE ADMINISTRATION

Washington, D.C. 20546